Global and Planetary Change 158 (2017) 119–133

Contents lists available at ScienceDirect

Global and Planetary Change

journal homepage: www.elsevier.com/locate/gloplacha

Planktic foraminiferal response to early Eocene carbon cycle perturbations in the southeast Atlantic Ocean (ODP Site 1263)

Valeria Luciani[a,*], Roberta D'Onofrio[a], Gerald R. Dickens[b], Bridget S. Wade[c]

[a] Department of Physics and Earth Sciences, Ferrara University, via G. Saragat 1, 44122, Italy
[b] Department of Earth Sciences, Rice University, Houston, TX 77005, USA
[c] Department of Earth Sciences, University College London, Gower Street, London, United Kingdom

ARTICLE INFO

Keywords:
Early Eocene Climatic Optimum
Planktic foraminiferal changes
Eocene carbon cycling
Bulk carbon isotopes

ABSTRACT

At low latitude locations in the northern hemisphere, striking changes in the relative abundances and diversity of the two dominant planktic foraminifera genera, *Morozovella* and *Acarinina*, are known to have occurred close to the Early Eocene Climatic Optimum (EECO; ~49–53 Ma). Lower Eocene carbonate-rich sediments at Ocean Drilling Program (ODP) Site 1263 were deposited on a bathymetric high (Walvis Ridge) at ~40° S, and afford an opportunity to examine such planktic foraminiferal assemblage changes in a temperate southern hemisphere setting. We present here quantified counts of early Eocene planktic foraminiferal assemblages from Hole 1263B, along with bulk sediment stable isotope analyses and proxy measurements for carbonate dissolution. The bulk sediment $\delta^{13}C$ record at Site 1263 resembles similar records generated elsewhere, such that known and inferred hyperthermal events can be readily identified. Although some carbonate dissolution has occurred, the well-preserved planktic foraminiferal assemblages mostly represent primary changes in environmental conditions. Our results document the permanent decrease in *Morozovella* abundance and increase in *Acarinina* abundance at the beginning of the EECO, although this switch occurred ~165 kyr after that at low-latitude northern hemisphere locations. This suggests that unfavourable environmental conditions for morozovellids at the start of the EECO, such as sustained passage of a temperature threshold or other changes in surface waters, occurred at lower latitudes first. The remarkable turnover from *Morozovella* to *Acarinina* was widely geographically widespread, although the causal mechanism remains elusive. In addition, at Site 1263, we document the virtual disappearance within the EECO of the biserial chiloguembelinids, commonly considered as inhabiting intermediate water depths, and a reduction in abundance of the thermocline-dwelling subbotinids. We interpret these changes as signals of subsurface water properties, perhaps warming, and the associated contraction of ecological niches.

1. Introduction

From a paleoclimate perspective, the early Paleogene represents an exceptionally interesting and dynamic time of Earth's history. Beginning about 59 million years ago (Ma), temperatures across Earth's surface slowly rose toward the Early Eocene Climatic Optimum (EECO), an extended interval of peak Cenozoic global warmth (Zachos et al., 2008). Average high-latitude and deep ocean temperatures during the EECO likely exceeded those at present day by at least 10 °C (Zachos et al., 2008; Bijl et al., 2009; Huber and Caballero, 2011; Hollis et al., 2012; Pross et al., 2012; Inglis et al., 2015). However, during the long-term early Paleogene warming and also within the EECO, our planet experienced several short-term (~40–200 kyr) global warming episodes, now referred to as hyperthermals (e.g., Kennett and Stott 1991; Thomas, et al., 2000; Lourens et al., 2005; Nicolo et al., 2007; Zachos et al., 2010; Coccioni et al., 2012; Kirtland-Turner et al., 2014; Littler et al., 2014; Lauretano et al., 2016).

Considerable scientific study has focused on understanding the early Paleogene hyperthermals, especially the most prominent example, the Paleocene-Eocene thermal maximum (PETM, ~56 Ma). This is because several of the hyperthermals were clearly associated with massive input of carbon to the ocean and atmosphere, as well as profound turnovers in various biotic ecosystems. The PETM has even been suggested as an outstanding past analogue for understanding current and future climate change (e.g., Dickens et al., 1997; Pagani et al., 2006; McInerney and Wing, 2011; Zeebe and Zachos, 2013). Less attention has been dedicated to the EECO and the long-lasting impacts of extraordinary global warmth, especially in terms of biotic response. In fact, a formal

* Corresponding author.
E-mail addresses: valeria.luciani@unife.it (V. Luciani), dnfrrt@unife.it (R. D'Onofrio), jerry@rice.edu (G.R. Dickens), b.wade@ucl.ac.uk (B.S. Wade).

http://dx.doi.org/10.1016/j.gloplacha.2017.09.007
Received 8 June 2017; Received in revised form 13 September 2017; Accepted 13 September 2017
Available online 15 September 2017

definition of EECO, first widely introduced by Zachos et al. (2001) based on the pronounced warming trend as expressed by a 1.5‰ decrease in the compiled $\delta^{18}O$ curve, remains problematic (Luciani et al., 2016). Recent workers (Slotnick et al., 2015; Lauretano et al., 2015; Luciani et al., 2016) have suggested resolving the terminology and stratigraphic issues by defining the EECO as the interval comprised between a significant carbon cycle perturbation known as the "J event" (Cramer et al., 2003) and the appearance of *Discoaster sublodoensis*, a well-calibrated and easily recognizable calcareous nannofossil biohorizon. The EECO thus spans from approximately 53 to 49 Ma, although average surface temperatures fluctuated during this time.

Significant plant and mammal turnovers occurred on land during the EECO (Wing et al., 1991; Zonneveld et al., 2000; Wilf et al., 2003; Falkowski et al., 2005; Woodburne et al., 2009; Figueirido et al., 2012). In the marine realm, evolutionary turnover happened as well, in particular the origin of modern calcareous nannofossil community structure (Agnini et al., 2006, 2014; Schneider et al., 2011; Shamrock et al., 2012) and possibly similarly for diatoms (Sims et al., 2006; Oreshkina, 2012). These observations, both from continents and the oceans, support a hypothesis that long-term climate change during the EECO may have impacted biotic evolution (Ezard et al., 2011).

Planktic foraminifera represent a fantastic class of organisms in which to examine links between past climate and evolution (e.g., Corfield, 1987; Kelly et al., 1996, 1998; Quillévéré and Norris, 2003; Ezard et al., 2011; Fraass et al., 2015). This is because they include numerous species, they precipitate carbonate tests, and they form a common component of many marine sediment records. A major turnover in planktic foraminifera occurred near the onset of the EECO (Luciani et al., 2016). This turnover involved two genera, *Morozovella* and *Acarinina*, which were important calcifiers of the tropical and subtropical early Paleogene oceans. More specifically, the abundance and diversity of *Morozovella* decreased significantly while the abundance and diversity of *Acarinina* increased significantly (e.g., Norris, 1991; Schmidt et al., 2004a; Berggren et al., 2006; Pearson et al., 2006; Aze et al., 2011; Fraass et al., 2015; Luciani et al., 2016). At multiple low-latitude locations in the northern hemisphere (Fig. 1), this "switch" in *Morozovella* and *Acarinina* genera happened rapidly and very close to the J event (Frontalini et al., 2016; Luciani et al., 2016). While tempting to suggest that the evolution of planktic foraminifera was crucially affected by the crossing of some critical threshold in surface water conditions at the start of the EECO, such as sustained elevated temperature, detailed records of planktic foraminiferal assemblages across this interval remain scarce (Fig. 1).

In this study, we examine planktic foraminiferal assemblages in lower Eocene sediment at Ocean Drilling Program (ODP) Site 1263 on Walvis Ridge in the southeast Atlantic Ocean (Fig. 1). Previous work on the lower Eocene interval at this site provides a solid and fairly detailed stratigraphic framework (e.g., Lourens et al., 2005; Westerhold et al., 2007; Stap et al., 2009, 2010a, 2010b; Lauretano et al., 2015, 2016), and shows that the carbonate-rich interval contains abundant and well-preserved planktic foraminifera (Shipboard Scientific Party, 2004). However, the planktic foraminiferal assemblages have not been studied at high-resolution. Site 1263 was probably located at ~40° S during the early Eocene (Van Hinsbergen et al., 2015). Consequently, the site presents an opportunity to view early Eocene planktic foraminiferal assemblage changes, especially the putative switch between morozovellids and acarininids, at a southern temperate location.

2. Materials and methods

2.1. ODP Site 1263: location, lithology and samples

Site 1263 is located in the southeast Atlantic (28°31.98′ S, 2°46.77′ E) and, at 2717 m below sea level (mbsl), a few hundred meters below the crest of Walvis Ridge (Zachos et al., 2004). Both the latitude and water depth of this site likely have changed over the Cenozoic. During the early Eocene, the location probably was positioned ~10° further south (Van Hinsbergen et al., 2015) (Fig. 1) and at a shallower depth of ~1500 mbsl (Zachos et al. 2004).

Three characteristics make the upper Paleocene and lower Eocene succession at Site 1263 especially amenable for foraminifera study. First, it was cored in four adjacent holes (1263A–1263D), so that core gaps and core overlaps can be ascertained (Shipboard Scientific Party, 2004; Westerhold et al., 2007, 2015). Second, for an open ocean setting, it is relatively thick but with minimal burial below the seafloor (Zachos et al. 2004). Third, it mainly consists of nannofossil ooze with good planktic foraminiferal preservation (Zachos et al. 2004). In short, the location contains an apparently complete and relatively expanded early

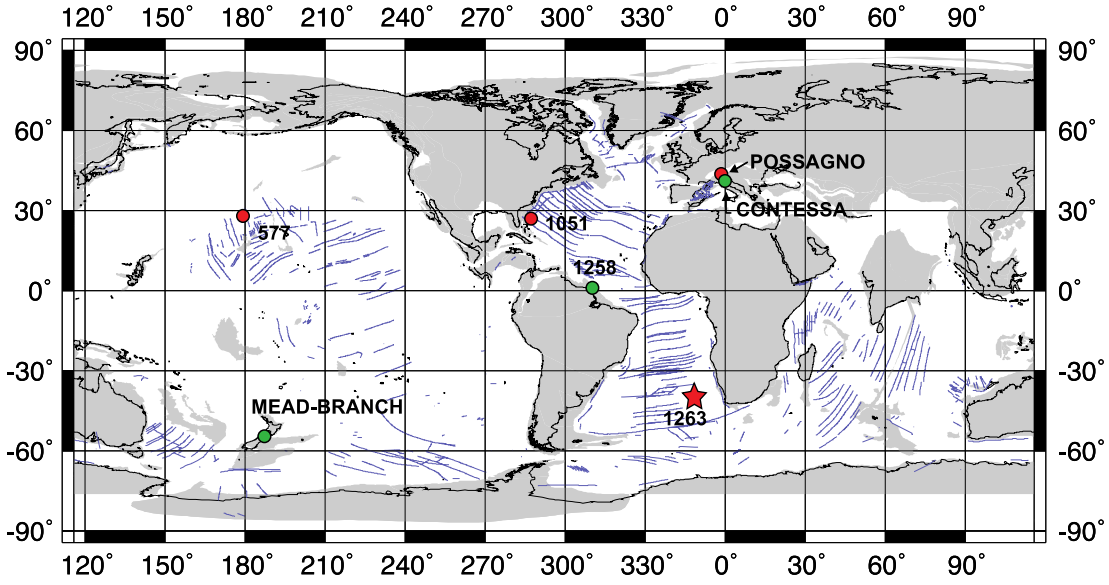

Fig. 1. Approximate location of the studied site (star) during the early Eocene. Also shown are other successions where detailed planktic foraminiferal records show a major change in genera across the EECO (red circles). We place two other locations because they have detailed $\delta^{13}C$ records across the EECO (green circles). Base map is from http://www.odsn/de/services/paleomap.html with paleolatitudes modified for Sites 577, 1051 and 1263 according to www.paleolatitude.org model version 1.2 (Van Hinsbergen et al., 2015). Early Eocene latitude for the Possagno section is based on the http://www.odsn.de/odsn/services/paleomap/adv_map.html mode, since they are not yet available at www.paleolatitude.org. (For interpretation of the references to colour in this figure legend, the reader is referred to the web version of this article.)

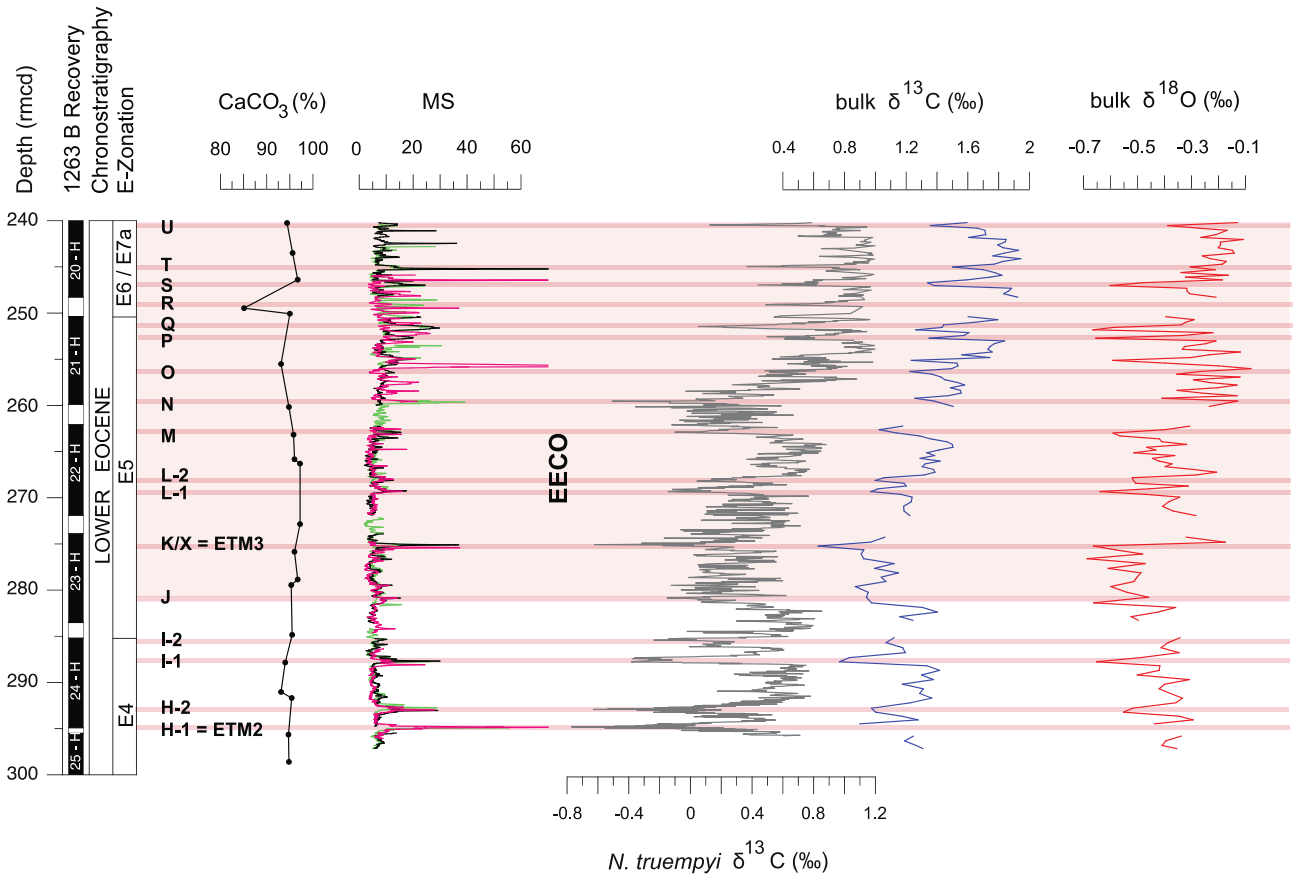

Fig. 2. Early Eocene carbonate content, magnetic susceptibility (MS) and stable isotope records at ODP Site 1263 on a revised composite depth (rmcd) scale. The bulk sediment $\delta^{13}C$ and $\delta^{18}O$ records are from this study (blue, light red) while the benthic foraminiferal (*N. truempyi*) $\delta^{13}C$ record comes from Lauretano et al. (2016) (grey). The magnetic susceptibility (MS) and the $CaCO_3$ content from the Shipboard Scientific Party (2004). The green, black and pink colors in the MS profile come from Holes 1263A, 1263B and 1263C, respectively. Planktic foraminiferal E-zonation follows Wade et al. (2011) as partly modified by Luciani and Giusberti (2014); the modifications are discussed in the text. Main carbon isotope excursions (CIEs) are labelled according to Lauretano et al. (2016). Pink lines help to identify the position of CIEs. The light pink shaded band defines the Early Eocene Climatic Optimum (EECO) interval as defined in recent papers (Lauretano et al., 2016; Luciani et al., 2016). (For interpretation of the references to colour in this figure legend, the reader is referred to the web version of this article.)

Eocene record with planktic foraminifera, one that accumulated with sedimentation rates between 10 and 30 m/Myr (Lauretano et al., 2016).

Consistent with a lower-bathyal open ocean depositional environment, lower Paleogene sediment at Site 1263 generally has high carbonate content ($CaCO_3$ ~ 90–95% by weight) (Fig. 2). However, these sediments also show pronounced variability at the dm- to m-scale, as clearly expressed in high-resolution magnetic susceptibility (MS) and colour reflectance data. These variations in physical properties principally relate to changes in carbonate content, with highs in MS reflecting lows in carbonate content. Some of the intervals with very high MS/low carbonate represent volcanic ash horizons, as confirmed by smear slide examination (Zachos et al., 2004). Importantly, though, other such intervals mark the established or suggested hyperthermal events (Zachos et al., 2005; Lourens et al., 2005; Stap et al., 2009, 2010a), which furthermore relate to extremes in eccentricity and precession (Westerhold et al., 2007; Zachos et al., 2010; Lauretano et al., 2015, 2016).

We adopt the revised composite depth (rmcd) scale provided by Westerhold et al. (2007, 2015) that combines depth records from cores at different holes. We thus sampled the interval between 297.16 and 240.21 rmcd at Hole 1263B. Given previous work at Site 1263, including alignment of physical property and stable isotope data (Lourens et al., 2005; Westerhold et al., 2007, Stap et al. 2009, 2010a, 2010b; Lauretano et al., 2015, 2016) and calcareous nannofossil and benthic foraminifera information across various hyperthermals (Dedert et al., 2012, 2014; Gibbs et al., 2012; D'haenens et al., 2014), our sampling spans several million years of the early Paleogene, especially including the J event and the start of the EECO.

2.2. Bulk sediment stable isotopes

A set of 140 samples, with a sampling resolution varying from ~30 cm to ~50 cm, were used to generate bulk sediment stable isotope records at Hole 1263B (Table S1). Samples were firstly freeze-dried and then pulverized manually in a mortar. Amounts of ~0.5 g of powdered samples were acidified at 50 °C to be analyzed. Bulk isotope analyses were performed at the UCL Bloomsbury Environmental Isotope Facility using the Gas Bench II and Cardiff University (UK) using a Thermo Finnigan MAT 252 mass spectrometer coupled with a Kiel III carbonate preparation device. Results are reported in conventional delta notation ($\delta^{13}C$ and $\delta^{18}O$) with reference to the Vienna Pee Dee Belemnite (VPDB) standard. An internal standard (with $\delta^{18}O = -2.43‰$ and $\delta^{13}C = 2.43‰$ versus VPDB) was measured between every sixth sample ensuring an analytical precision within 0.04 and 0.08‰ for $\delta^{13}C$ and $\delta^{18}O$ respectively. Additional duplicate analyses were conducted on 9 selected samples giving reproducibility better than 0.1 for $\delta^{13}C$ and 0.2‰ for $\delta^{18}O$.

2.3. Proxies for carbonate dissolution

Extreme global warming episodes that characterized the early Eocene were marked by low carbonate contents in deep-sea settings

(e.g., Zachos et al., 2005; Stap et al., 2009; Leon-Rodriguez and Dickens, 2010). This correspondence, which is apparent in MS records from Walvis Ridge sections (Fig. 2), once ash horizons are discounted, has been attributed principally to carbonate dissolution relating to massive and rapid carbon into the ocean and atmosphere during the hyperthermals, because this would reduce carbonate saturation horizons (Dickens et al., 1997; Kump et al., 2009; Zeebe et al., 2009). This is important to realize when examining early Paleogene planktic foraminiferal assemblages, because their tests are differentially prone to dissolution and more so than both benthic foraminifera tests and most calcareous nannofossils (Berger, 1970; Bé et al., 1975; Thunell and Honjo, 1981; Hancock and Dickens, 2005; Petrizzo et al., 2008; Nguyen et al., 2009, 2011; Leon-Rodriguez and Dickens, 2010; Nguyen and Speijer, 2014). Dissolution can therefore modify the composition of planktic foraminiferal assemblages significantly. On the other hand, the decreases in carbonate content may also relate to decreased carbonate production in surface waters and ensuing carbonate rain to the seafloor, as highlighted recently for the PETM (Luo et al., 2016).

To evaluate possible dissolution effects across the studied section at Site 1263, we chose three different proxies (detailed below). These proxy measurements were determined on 75 samples. The sample spacing varied between 30 and 40 cm across several major carbon cycle perturbations, and from 40 cm to 1 m through remaining intervals (Table S1). The proxies are:

(1) The fragmentation index (*F index*). Planktonic foraminifera tend to break into fragments when they begin to dissolve (Berger, 1970, 1973; Bé et al., 1975; Leon-Rodriguez and Dickens, 2010; Nguyen and Speijer, 2014). Consequently, fragmentation is a commonly adopted proxy for planktic foraminiferal dissolution. The *F index* (expressed as a percentage) was calculated here according to Berger (1970): the ratio between fragments or partially dissolved planktic foraminiferal tests versus entire tests on ~300 elements. Amongst the fragmented tests, we included all planktic foraminiferal specimens showing missing or deteriorated chambers and substantial breakage.
(2) The planktic over benthic (P/B) ratio. Most planktic foraminifera preferentially dissolve relative to benthic foraminifera. The P/B ratio, often adopted for paleobathymetric estimates (e.g., Murray, 1976; Van der Zwaan et al., 1990), therefore also can be applied as a dissolution index (e.g., Hancock and Dickens, 2005; Nguyen et al., 2009; Nguyen and Speijer, 2014). The *P/B index* was here calculated on ~300 whole specimens and is expressed as $100 * P / (P + B)$.
(3) The weight percent coarse fraction (*WPCF*). Planktic foraminifera, including "juvenile" specimens, generally exceed 38 μm. Dissolution of planktic foraminifera, such as observed with seafloor sediment within the lysocline, thus modifies bulk sediment grain size (e.g., Berger et al., 1982). The *WPCF* was calculated as the ratio between the weights of the dry fraction ≥ 38 μm and the bulk dry sediment (Hancock and Dickens, 2005).

All three parameters come with caveats (Hancock and Dickens, 2005). For example, an increase in calcareous nannofossil production will affect the *WPCF*, and an increase in planktic foraminiferal production will affect the *WPCF* and *P/B index*.

2.4. Planktic foraminiferal distribution and abundances

We collected data on planktic foraminifera for the same 75 samples at Hole 1263B used to generate dissolution proxies (Table S1). Planktic foraminifera were studied on washed residues using a stereomicroscope with an incident light beam. The residues were prepared by immersing previously freeze-dried bulk samples in deionized water. Disaggregation occurred in a time varying from few hours to three days, depending on the compactness of the sediments. When disaggregated, samples were washed over stacked > 63 and > 38 μm sieves. After each washing, sieves were immerged in a methylene blue bath in order to colour planktic foraminifera potentially trapped in the sieve mesh (e.g., Green, 2001). This is an easy method to exclude possible contaminations amongst different samples. The separated fractions of each washed residue were dried at < 50 °C.

The taxonomic criteria adopted to identify planktic foraminiferal genera and species follow Pearson et al. (2006, and references therein). Relative abundances of planktic foraminiferal genera were generated at Site 1263 by counting at least 300 complete specimens in random splits from the ≥ 63 μm size fractions and are expressed in percentages. Some foraminiferal genera were grouped according to their similar depth habitat as reported by Pearson et al. (2006, and references therein). Accordingly, the *Subbotina* group includes the genera *Subbotina* and *Parasubbotina*, and the chiloguembelinids comprise the genera *Chiloguembelina* and *Zeauvigerina*. We keep separate the species *Subbotina senni*, since this taxon occupied a different habitat with respect to the other subbotinids. Specifically, this species is considered a mixed-layer form that sank to middle mixed-layer or deeper depths during gametogenesis (Pearson et al., 1993; Pearson et al., 2006 and references therein).

2.5. Chronology

Using high-resolution variations in sediment composition, including benthic foraminifera stable isotopes, Lauretano et al. (2016) presented a detailed astronomically tuned age model for the lower Eocene interval at Site 1263. We use this age model, which places the J event (280.85 rmcd) at 53.27 Ma.

3. Results and discussion

3.1. Bulk carbon isotope records

The bulk sediment $\delta^{13}C$ record (Fig. 2, Table S1) exhibits both trends and excursions. In the basal part of the studied interval (297.16 to 281.87 rmcd), $\delta^{13}C$ values average ~ 1.2‰ with no clear trend. Bulk sediment carbon isotope values generally decrease by ~0.25‰ between 280.77 and 274.25 rmcd. The $\delta^{13}C$ values gradually increase above this interval, reaching a maximum of ~1.9‰ in the uppermost part of the investigated interval. High-frequency $\delta^{13}C$ variations are superimposed on these basic trends, most obviously multiple negative carbon isotope excursions (CIEs) with magnitudes ranging from 0.4‰ to 0.7‰ (Fig. 2, Table S1).

Although the absolute values of $\delta^{13}C$ vary, both the trends and CIEs have been observed in other $\delta^{13}C$ records spanning all or part of the EECO. This includes bulk sediment $\delta^{13}C$ records at the neighbouring ODP Site 1262 (Walvis Ridge, Zachos et al. 2010), ODP Site 1258 (Demerara Rise, west equatorial Atlantic, Kirtland-Turner et al., 2014), ODP Site 1051 (Blake Nose, northwest Atlantic, Luciani et al., in press), DSDP Site 577 (Shatsky Rise, northwest Pacific, Luciani et al., 2016), and the Branch and Mead Stream sections in New Zealand (Slotnick et al. 2012, 2015). Importantly, the correspondence also can be observed in the benthic foraminiferal (*Nuttallides truempyi*) $\delta^{13}C$ record at Site 1263 (Lauretano et al., 2016) (Figs. 2, 3). The variations in $\delta^{13}C$ through the early Eocene are truly global and signify changes in the composition of dissolved inorganic carbon (DIC) pools of the ocean. We note the ~1‰ offset in absolute $\delta^{13}C$ values between the bulk and benthic foraminifera records, which principally reflects differences between surface and deep ocean DIC composition as well as differences between carbon isotope fractionation by calcareous nannofossils and benthic foraminifera.

We interpret and label the primary CIEs following Coccioni et al. (2012) and Lauretano et al. (2016), who extended the alphabetic ordering scheme initiated by Cramer et al. (2003) to a bulk sediment $\delta^{13}C$ record in Italy and to the benthic foraminiferal $\delta^{13}C$ record at Site 1263.

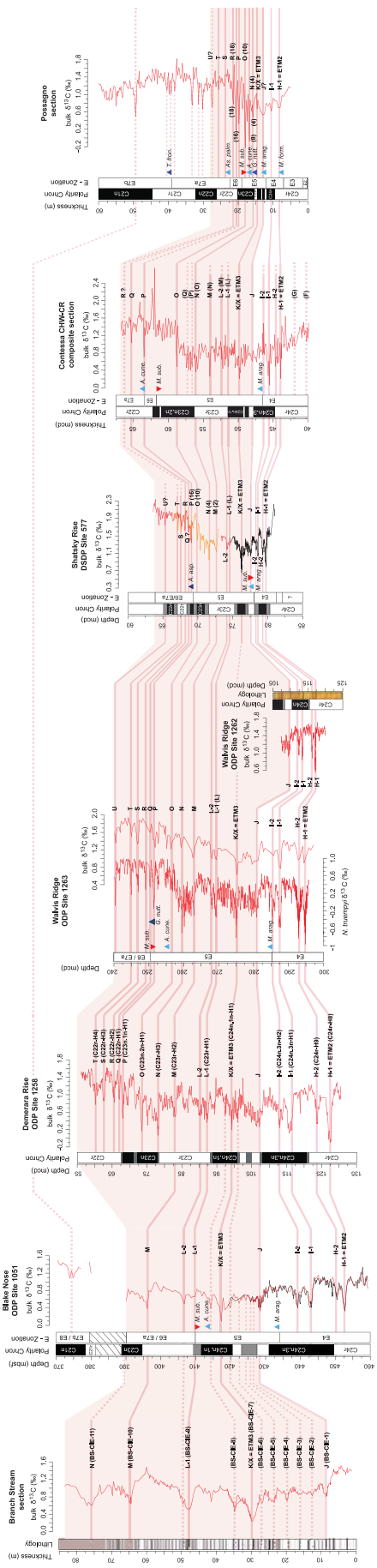

Fig. 3. Correlation of carbon isotope records spanning the early Eocene from several global sites (see Fig. 1). These are: Branch Stream (New Zealand, Slotnick et al., 2015), ODP Site 1051 (Blake Nose, Cramer et al., 2003; Luciani et al., 2016, in press), Site 1258 (Demerara Rise, Kirtland-Turner et al., 2014), Site 1263 (Walvis Ridge, Lauretano et al., 2016, this study), Site 1262 (Walvis Ridge, Zachos et al., 2010), DSDP Site 577 (Shatsky Rise, Cramer et al., 2003; Luciani et al., 2016), Contessa Road (central Italy, Coccioni et al., 2012) and Possagno (north-eastern Italy, Luciani et al., 2016). Where possible, magnetostratigraphy, lithology and planktic foraminiferal zonation are given. Zonal schemes are from Wade et al. (2011) as modified by Luciani and Giusberti (2014; see text) for Blake Nose, Walvis Ridge, Shatsky Rise, Possagno section and from Wade et al. (2011) for the Contessa CHW-CR. Records from Sites 577 and 1051 are in two colors: black (Cramer et al., 2003), which ended at the start of the EECO, and orange/red for newer data (Luciani et al., 2016, unpublished) that extended the records through the EECO. Carbon isotope excursions (CIEs) are highlighted with pink lines and labelled following Lauretano et al. (2016). Original labels used by different authors are shown in brackets. Dashed bands indicate events not consistently correlated. Correlation problems are mainly related to different resolution of $\delta^{13}C$ records and sedimentation rates. The light pink shaded band defines the Early Eocene Climatic Optimum (EECO) interval as denoted in Fig. 2. Main planktic foraminiferal events are shown as light-blue triangles (bases), dark-blue triangles (bases rare) and red triangles (tops). *M. form.* = *Morozovella formosa*; *M. arag.* = *Morozovella aragonensis*; *A. cune.* = *Acarinina cuneicamerata*; *A. asp.* = *Acarinina aspensis*; *M. sub.* = *Morozovella subbotinae*; *As. pal.* = *Astrorotalia palmerae*; *G. nutt.* = *Guembelitrioides nuttalli*; *T. fron.* = *Turborotalia frontosa*. Modified from Luciani et al. (unpublished). (For interpretation of the references to colour in this figure legend, the reader is referred to the web version of this article.)

The minimum value of ~0.6‰ at 275.22 rmcd corresponds to the K/X (or ETM3) event. We recognize below this horizon the Eocene Thermal Maximum 2 (ETM2 or H-1), H-2, I-1, I-2, and J events, and above this horizon the L to U events (Fig. 2). This template allows us to accurately identify the stratigraphic position of biotic events, even where core gaps exist in Hole 1263B, such as proximal to the ETM2, I-2, M, R and the U events.

Most of the documented CIEs at Site 1263 correspond to peaks in MS (Shipboard Scientific Party, 2004), although the magnitudes of peaks in MS are not proportional to the magnitudes of CIEs because some MS peaks correspond to ash horizons (Fig. 2). The O and T events, for example, have relatively small CIEs, but marked peaks in MS (> 60), whereas the J, M and L-1 events display low values in MS (< 30), despite relatively large CIEs.

3.2. Bulk oxygen isotope records

The bulk sediment oxygen isotopes at Hole 1263B (Fig. 2, Table S1) vary between − 0.1‰ and − 0.7‰, with an average value of − 0.36‰. Oxygen isotope values show a slight and gradual decrease in values from the base of the investigated interval to the K/X event. Immediately above the K/X event, bulk sediment $\delta^{18}O$ values increase by about 0.4‰. The $\delta^{18}O$ values then oscillate around a mean value of ~ − 0.3‰ through the top of the investigated interval. Superimposed on these general trends are a series of negative $\delta^{18}O$ excursions that reach values of ~ − 0.7‰. These appear to strictly correlate with the identified CIEs (Fig. 2).

Similar trends have been observed in other bulk $\delta^{18}O$ profiles (Possagno section, Luciani et al., 2016; Site 1258, Kirtland-Turner et al., 2014; Site 577, Luciani et al., 2016; Site 1051, Luciani et al., in press), although they have different absolute values. As noted below, planktic foraminifera at Site 1263 exhibit a "frosty" texture (sensu Sexton et al., 2006). Moreover, discoasterids in the studied section commonly have calcite overgrowths (Shipboard Scientific Party, 2004). These observations imply some degree of recrystallization in bulk sediment, which presumably occurred at or beneath the seafloor (e.g., Pearson et al. 2001; Sexton et al. 2006; Pearson, 2012). Bulk sediment $\delta^{18}O$ records are complicated as a proxy for temperature because they represent mixtures of different components that fractionate ^{18}O differently (e.g., Reghellin et al., 2013). Moreover, diagenetic alteration impacts the complex original ^{18}O signal further, because temperatures on the seafloor and over the upper few hundred meters of seafloor are generally colder than near surface waters where most tests precipitated (Schrag et al., 1995; Pearson et al., 2001; Stap et al., 2010a; Kozdon et al., 2011).

Absolute temperature estimates made from the bulk $\delta^{18}O$ record at Site 1263 would be difficult to justify. Nevertheless, even though recrystallization may have shifted our $\delta^{18}O$ values, the CIEs manifest in our $\delta^{18}O$ data so that the main patterns remain. This can be explained by a twofold mechanism. First, the CIEs represent hyperthermals, when surface water temperatures were significantly warmer than surrounding time intervals, or biological constituents with lower $\delta^{18}O$ were significantly more abundant than surrounding time intervals. Second, diagenesis involving carbonate dissolution and recrystallization occurred at a very local scale (< 1 m) (Schlanger and Douglas, 1974; Matter et al., 1975; Arthur et al., 1984; Kroenke et al., 1991; Borre and Fabricus, 1998; Frank et al., 1999; Slotnick et al., 2015), so that the short-term $\delta^{18}O$ anomalies remain.

3.3. Variations in dissolution and productivity proxies

The *F index* record exhibits minimum values of ~10% and oscillates around a mean value of ~32% (Fig. 4, Table S2). Importantly, the major peaks in *F index* coincide with the prominent CIEs. In our record, the ETM2, I1, J, K/X, L, M, P and S events have, respectively, *F index* values of 54%, 52%, 63%, 45%, 44%, 90%, 51% and 58%. However, the magnitudes of the CIEs and MS peaks are not proportional with the amplitudes of the *F index* peaks, in the latter case because the peaks are linked to ash layers (Shipboard Scientific Party, 2004).

The *P/B index* profile shows relatively constant values throughout the early Eocene, averaging ~97%. Minor reductions to 92% and 88% coincide with the J and the M events, respectively (Fig. 4, Table S2).

The *WPCF* fluctuates between ~0.02% and ~2.6%, varying around a mean value of ~1.4% (Fig. 4, Table S2). However, a modest decrease in mean *WPCF* occurs through the investigated interval, so that values move from ~1.6% in the interval below the paired L events to ~1.2% within the main phase of the EECO. High-frequency changes in the *WPCF* record do not correlate very well with the CIEs, although a decrease of ~1% happens across the M event, which coincides with the highest *F index*.

3.4. Planktic foraminiferal biostratigraphy

Planktic foraminifera generally comprise < 5% of the total sediment, consistent with Zachos et al. (2004), but numerous and diverse specimens were extracted from all samples investigated. Although the tests show classic "frosty" preservation, sensu Sexton et al. (2006), they are well preserved, allowing unambiguous identification at the species level. The main early Eocene planktic foraminiferal biohorizons, as defined by bases (B) or tops (T) of species in the Wade et al. (2011) zonal scheme, can be identified at Site 1263 (Plate 1). However, there are some differences, as noted by Luciani and Giusberti (2014) and described below.

Base of *Morozovella aragonensis*: This datum, that identifies the E4/E5 boundary (Wade et al., 2011), is found at 285.69 ± 0.45 rmcd, slightly above the I-2 event (Fig. 3) as in the Tethyan Contessa section (Coccioni et al., 2012). At ODP Site 1051, DSDP Site 577 and the Tethyan Possagno section, this horizon also lies above the I-2 event, although perhaps slightly higher (Lu and Keller, 1995; Luciani et al., 2016; unpublished). Some uncertainty may lie with the B of *M. aragonensis* because of subtle differences between the identification of true *M. aragonensis* and its ancestor *M. lensiformis*, that could give rise to apparent diachronism (Pearson et al., 2006). We recognize here *M. aragonensis* from *M. lensiformis* by its truly plano-convex test, truncated-cone shape, and rounded peripheral outline (Plate 1). We noted that typical *M. aragonensis* mainly presents 5.5–6 chambers in the last whorl, according to what observed by Luciani and Giusberti (2014).

Base of *Acarinina cuneicamerata*: This datum, which is supposed to mark the E6/E7a boundary (Wade et al., 2011), is found at 256.32 ± 0.30 rmcd, just above the O CIE and below the T of *M. subbotinae* (Fig. 3). Thus, there is a stratigraphic problem, because the B of *A. cuneicamerata* should occur above the T of *M. subbotinae* according to the Wade et al. (2011) zonal scheme and consistent with the record from the Contessa section (Coccioni et al., 2012). The data at Site 1263 confirms the record from the Possagno section and Atlantic Site 1051 (Luciani and Giusberti, 2014) where the B of *A. cuneicamerata* and the T of *M. subbotinae* also occur in reversed order. Conversely, at Site 1051 and at the Possagno section the B of *A. cuneicamerata* occurs earlier with respect to Site 1263 as it is recorded between the K/X and L events (at the CIE labelled as CIE6b) and just above the O event respectively (Fig. 3). Given the diachroneity of this bioevent, Luciani and Giusberti (2014) tentatively proposed the B of *Astrorotalia* (*Planorotalites*) *palmerae* as an alternative marker for the E6/E7a boundary. However, *A. palmerae* is absent at Site 1263 and therefore we combine together Zones E6 and E7a. The first specimens of *A. cuneicamerata* at Site 1263 are rare but typical specimens (Plate 1) and evenly distributed through adjacent samples.

Base of *Guembelitrioides nuttalli*: This datum, which should set the E7b/E8 boundary, somewhat above the base of the middle Eocene (Wade et al., 2011; Molina et al., 2011), is found at 251.55 ± 0.29 rmcd and slightly above the Q CIE. Again, there is a stratigraphic issue at the studied section. However, the observation at

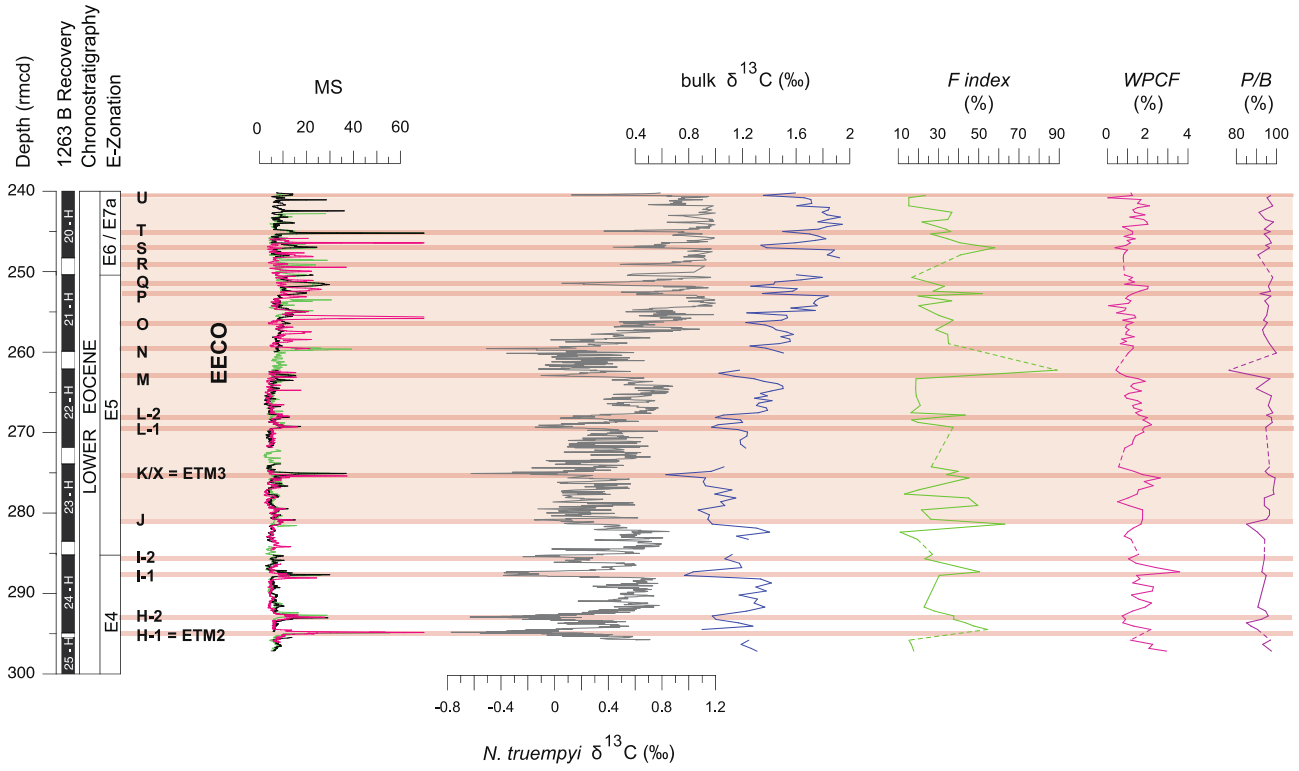

Fig. 4. Early Eocene $\delta^{13}C$, dissolution proxy and MS records at ODP Site 1263. Bulk sediment $\delta^{13}C$ from this study (blue), and benthic foraminiferal *N. truempyi* $\delta^{13}C$ from Lauretano et al. (2016) (grey). Dissolution proxy records: fragmentation index (F index), weight percent coarse fraction (WPCF), and planktic over benthic ratio (P/B). Other information is consistent with Fig. 2. MS record from Shipboard Scientific Party (2004). (For interpretation of the references to colour in this figure legend, the reader is referred to the web version of this article.)

Site 1263 confirms the early first appearance of this species as documented by Luciani and Giusberti (2014) for the Tethyan Possagno section. Luciani and Giusberti (2014) noticed that, at Possagno, the abundance of *Guembelitroides nuttalli* varied significantly, such that there is a Base of rare specimens (Br, < 1%) and a Base of common (Bc, ~4%) specimens, where the latter coincides with the base of Zone E8. The Br of *G. nuttalli* at Site 1263 is, however, seemingly at a significantly higher stratigraphic position than recorded at Possagno (Fig. 3) (Luciani and Giusberti, 2014). *Guembelitroides nuttalli* at Site 1263 are typical specimens (Plate 1) but very rare up to the top of the studied succession (Fig. 5).

Top of *Morozovella subbotinae*: This event, which marks the base of Zone E6 (Wade et al., 2011), occurs at 251.00 ± 0.27 rmcd and slightly above the Q CIE. At the Contessa section, this bioevent occurs within chron C23n.1n, and between the O and P events (Coccioni et al., 2012) similarly to the Possagno section. At Site 1051, the T of *M. subbotinae* was recorded in a significantly lower position, as it coincides with the L2 event, at the base of C23r (Luciani et al., 2016) (Fig. 3). At Site 577, the top of *M. subbotinae* occurs even earlier, in the middle of C24n (Lu and Keller, 1995), so the E5–E6 boundary was tentatively positioned at the lowest occurrence of *Acarinina aspensis* (Luciani et al., 2016), according to the original definition of Zone E5 (Berggren and Pearson, 2005). Luciani et al. (2016) emphasized the significant diachronism of this event. However, in absence of a revision of the Wade et al. (2011) zonal scheme, the T of *M. subbotinae* is still the present marker for the base of Zone E6. At Site 1263, the specimens of this taxon are relatively small in the final interval of their occurrence.

3.5. Variations in planktic foraminiferal abundances

The early Eocene planktic foraminiferal assemblages display both long-term and transient changes across the investigated interval at Site 1263 (Fig. 5, Table S3). Major changes involve the mixed-layer dwelling warm-index acarininids and morozovellids (e.g., Boersma et al., 1987; Pearson et al., 1993, 2006), which collectively represent the most abundant planktic foraminiferal taxa throughout. The most prominent change, which occurs between the J and K/X events, involves a strong and permanent reduction in morozovellid abundances from a mean value of ~23% in samples below ~278 rmcd to a mean value of ~9% in samples above (Fig. 5). Moreover, qualitative observation regarding the *Morozovella* species distribution reveals that, in the pre-EECO interval, *M. aequa* and *M. subbotinae* were the dominant taxa, *M. lensiformis* and *M. crater* were relatively common, and *M. formosa*, *M. gracilis* and *M. marginodentata* were quite rare. Within the EECO, *M. aragonensis* and *M. crater* become the most common taxa along with moderate occurrences of *M. aequa*, *M. formosa*, and *M. lensiformis*. The species *M. gracilis*, *M. marginodentata* and *M. subbotinae* progressively decrease in abundance and disappear within the EECO. On the basis of these evidences, the reductions in abundance of *M. aequa*, *M. subbotinae* and secondarily of *M. lensiformis* and *M. crater*, mainly contributed to the morozovellid collapse, although a quantitative count for the *Morozovella* species is necessary to confirm this observation. A rather different pattern has been recorded at the northern Atlantic Site 1051 where *M. gracilis*, *M. lensiformis*, *M. marginodentata* and *M. subbotinae* were dominant before the J event, and large reduction in the abundance of these four species, which ultimately disappeared within the EECO, give rise to the major morozovellid collapse (Luciani et al., unpublished). This pattern is interesting because shows that the permanent morozovellid decline in abundance involved differently the *Morozovella* species at different sites.

Notably, the morozovellid test size appears reduced within the EECO at Site 1263 above the major drop in abundance. This is especially evident in the > 250 μm fraction for *M. lensiformis*, *M. subbotinae*, *M. aequa* and secondarily for *M. gracilis* and *M. marginodentata*. A decrease in test size has also been recorded for *M. lensiformis*, *M. marginodentata* and *M. gracilis* at the tropical Atlantic Site 1051 above their permanent decline in abundance (Luciani et al., unpublished).

In contrast to the morozovellid trend, the relative abundance and

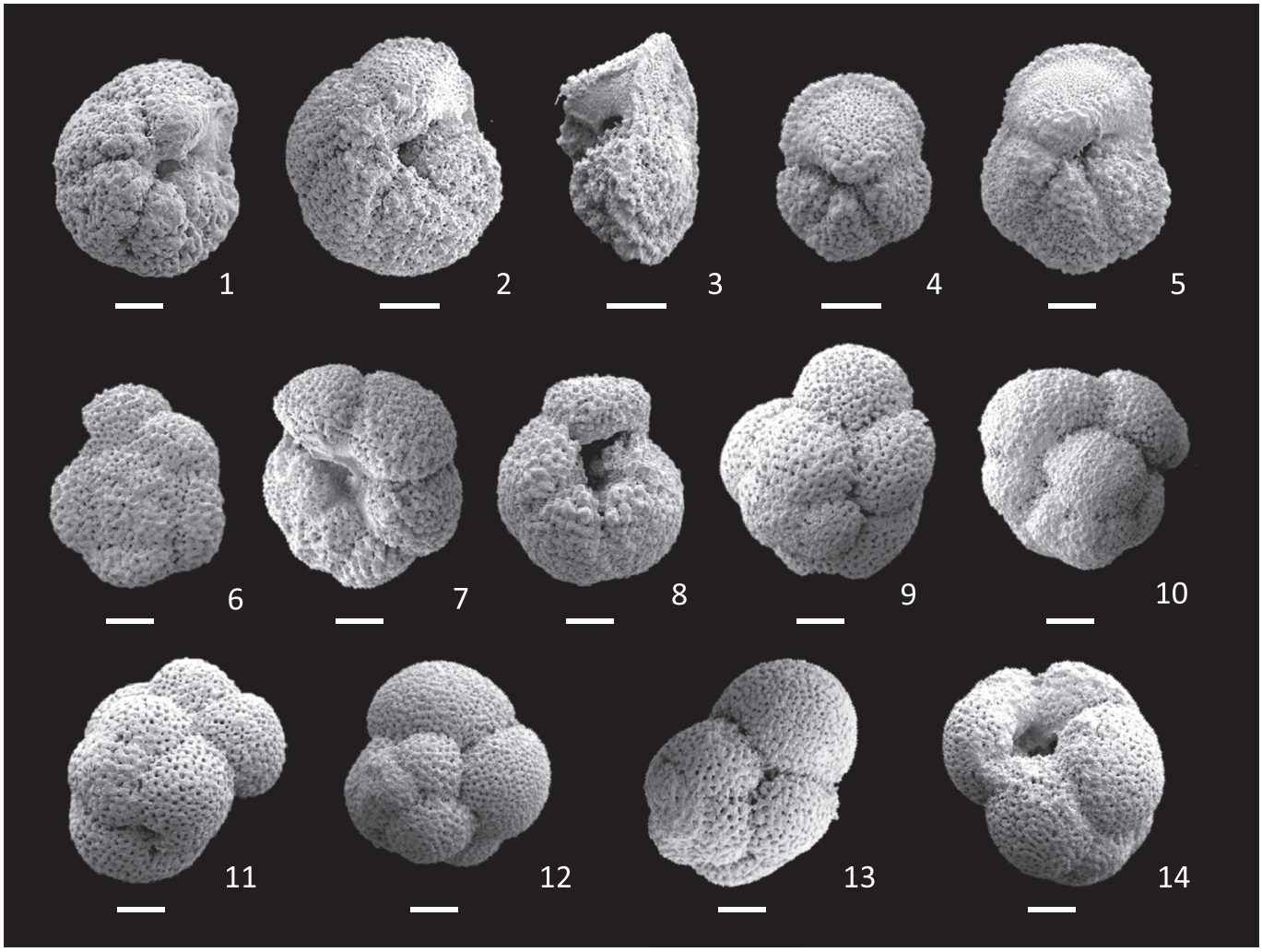

Plate 1. Scanning electron micrograph (SEM) images of the zonal markers from the early Eocene interval here analyzed at Site 1263. 1–3: *Morozovella aragonensis* (Nuttal, 1930); 1 sample 251.28 rmcd (Hole 1263B, 21H-1, 90–92 cm), 2–4 sample 251.01 rmcd (Hole 1263B, 21H-1, 60–62 cm). 4–5: *Morozovella subbotinae* (Morozova, 1939), 4 sample 251.01 rmcd (Hole 1263B, 21H-1, 60–62 cm), 5 sample 258.09 rmcd (Hole 1263B, 21H-6, 30–32 cm). 6–8: *Acarinina cuneicamerata* (Blow, 1979); 6–7 sample 255.42 rmcd (Hole 1263B, 21H-4, 60–62 cm), 8 sample 251.01 rmcd (Hole 1263B, 21H-1, 60–62 cm). 9–14: *Guembelitrioides nuttalli* (Hamilton, 1953); 9 sample 251.28 rmcd (Hole 1263B, 21H-1, 90–92 cm), 10 sample 251.01 rmcd (Hole 1263B, 21H-1, 60–62 cm), 11 sample 242.61 rmcd (Hole 1263B, 20H-3, 100–102 cm), 12–13 sample 251.01 rmcd (Hole 1263B, 21H-1, 60–62 cm), 14 sample 242.61 rmcd (Hole 1263B, 20H-3, 100–102 cm). Scale bars: 100 μm.

diversity of acarininids increases upward. *Acarinina* comprise ~53% of assemblages in the pre-EECO interval below the K/X event, but comprise ~75% above this event. The species *A. coalingensis* and *A. soldadoensis* are the dominant taxa throughout. However, *A. interposita*, *A. esnaensis* and *A. wilcoxensis* are relatively common in the pre-EECO interval, whereas *A. cuneicamerata*, *A. primitiva* and *A. quetra* become more common in the upper part of the investigated interval.

In the studied interval at Site 1263, a long-term reduction in subbotinid abundance (dominated by *Subbotina* with respect to *Parasubbotina*) happens across the EECO, whereby the mean value of their abundance in assemblages drops from ~16% to ~9%. Much of this change occurs above the paired L events, specifically around 266.63 rmcd (Fig. 5, Table S3).

The three dominant taxa also display high-frequency variations in abundance superimposed on long-term trends. At a basic level, short-term fluctuations in the abundance of *Acarinina* coincide with contrasting abundance changes of *Morozovella* and subbotinids. This relationship is particularly evident across the CIEs, where acarininid abundances generally increase to comprise > 70% of the total assemblage. Most prominent is the peak of ~90% acarininid abundance across the paired L events. Interestingly, abundances of morozovellids and subbotinids often recover rapidly above the CIEs (Fig. 5). Here, of course, it should be recognized that the above changes in abundances reflect a closed-sum effect, where the drop in one genus necessarily relates to a rise in one or more other genera. However, the acarininid dominance across the CIEs appears as a real response to the hyperthermals in the mixed layer, as documented also in several Tethyan successions (see discussion in Section 3.6).

A major and permanent drop in the chiloguembelinid group (dominated by *Chiloguembelina* with respect to *Zeauvigerina*) occurs at the start of the EECO (Fig. 5, Table S3). Mean abundances of this group are ~10% in the pre-EECO interval but approach zero above the K/X event. The genera *Igorina*, *Planorotalites*, *Globanomalina*, *Catapsydrax* and the species *Guembelitriodes nuttalli* are very rare in the assemblages throughout the early Eocene, and never exceed 5% in terms of total planktonic foraminifera abundance. These forms do not display significant variations within the investigated interval.

3.6. The foraminiferal record across the EECO at Site 1263

3.6.1. Low carbonate dissolution and decreased planktic foraminiferal productivity

The minor long-term variability displayed by the three dissolution proxies (Fig. 4) suggests that broad features in the evolution of

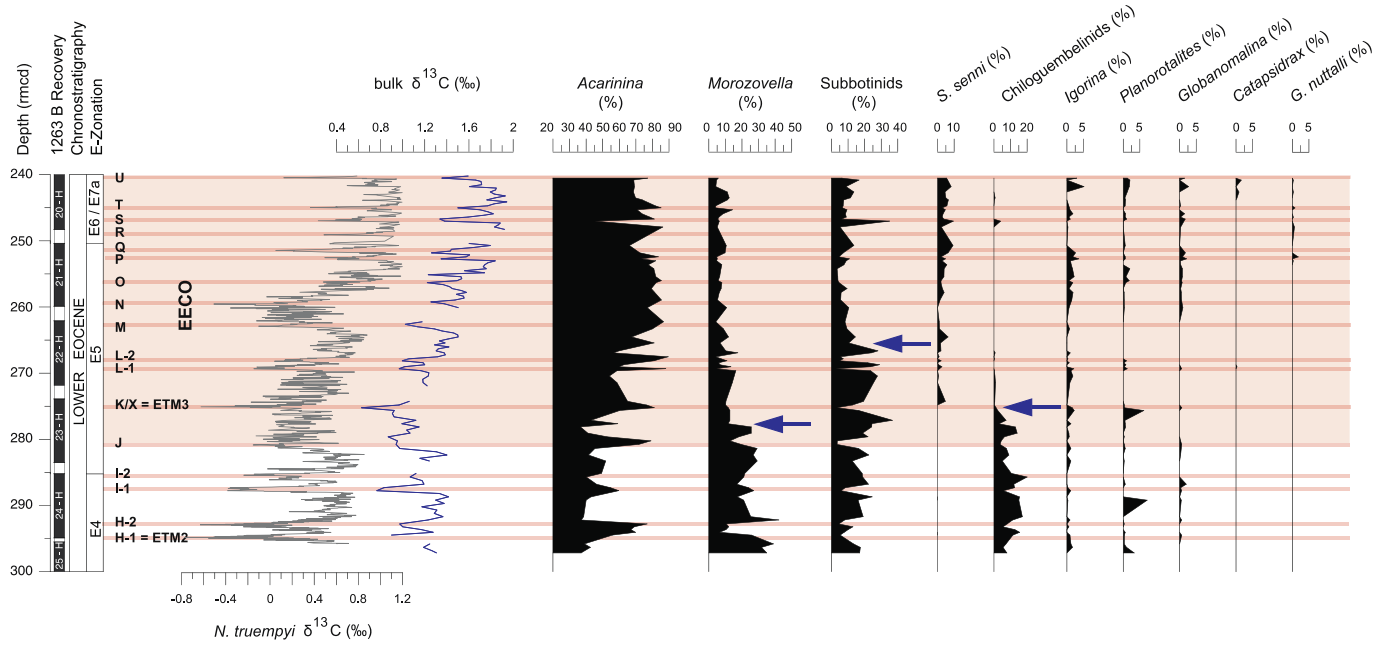

Fig. 5. Relative abundances of planktic foraminiferal genera across the early Eocene interval at ODP Site 1263. Subbotinids include the genera *Subbotina* (dominant) and *Parasubbotina* that are known as having similar depth habitat (e.g., Pearson et al. 2006, and references therein). Chiloguembelinids include the genera *Chiloguembelina* (dominant) and *Zeauvigerina* (very rare). Note: (1) the major switch in *Morozovella* abundance slightly above the J event; (2) the decrease in subbotinids above the paired L events; (3) the virtual disappearance of chiloguembelinids above the K/X event. Other information is consistent with Fig. 2.

foraminiferal assemblages represent genuine biotic trends rather than selective dissolution. The *F-index* rises across some of CIEs, although these increases do not proportionally correspond to CIE intensity. In fact, the highest *F-index* value corresponds with the relatively modest M CIE (Fig. 4). A small decrease in the *P/B index* across the M CIE may denote that this horizon experienced some dissolution. Variations in the abundances of planktic foraminiferal genera at Site 1263 do not clearly correspond to dissolution indices. This finding is consistent with locations where CIEs have with low *F-index* and major increases of *Acarinina* (Luciani et al., 2016). For example, at the Tethyan Terche section in northern Italy, D'Onofrio et al. (2014, 2016) noted pronounced spikes in *Acarinina* abundance at the ETM2, H1 and I-2 events where planktic foraminiferal assemblages do not seem biased by dissolution. We suggest that carbonate dissolution at or beneath the seafloor at Site 1263 may have partly amplified changes in planktic foraminiferal assemblages, but that the changes mainly reflect variations in the rain of tests from surface water. This makes sense, given the shallow setting of Site 1263 during the early Eocene and the limited burial depth since.

Given the low impact of dissolution inferred by the *F-index* and *P/B index*, the long-term decease in *WPCF* (Fig. 4) can be interpreted as a signal of decreased planktic foraminiferal productivity, relative to calcareous nannoplankton productivity. Here we note that the total carbonate content averages about 95%, the *WPCF* averages about 1.4%, and shipboard smear slides show that calcareous nannofossils dominate the bulk sediment (typically > 90%). This implies that the vast majority (> 90%) of the total sediment and total carbonate reaching the seafloor consisted of calcareous nannofossils. Thus, a 50% change in the flux of calcareous nannofossils to the seafloor would significantly change the sedimentation rate and moderately affect the carbonate content, whereas a 50% change in the flux of foraminiferal tests to the seafloor would mostly affect the *WPCF*.

The overall long-term sedimentation rate decreased from ~20 m/Myr to ~10 m/Myr at about 52 ± 1 Ma (Zachos et al., 2004). The simplest explanation for the above observations is that carbonate fluxes to the seafloor at the location of Site 1263 decreased within the EECO, but this was more pronounced (on a percentage basis) for the planktonic foraminifera. The long-term reduction in foraminifera supply may be linked to the drop in *Morozovella* abundance, since the decline in subbotinids was somewhat balanced by an increase in the abundance of *Subbotina senni* (Fig. 5). A similar decrease in planktic foraminiferal productivity has been suggested for the Tethyan Possagno section during the EECO and also related to the decrease in morozovellid abundance (Luciani et al., 2016).

3.6.2. The permanent Morozovella and Acarinina switch in abundances at the EECO onset

Our records provide new insight on the impact of the EECO upon planktic foraminiferal genera that characterized early Paleogene assemblages. The integrated biotic and $\delta^{13}C$ stratigraphy allows us to relate the planktic foraminiferal assemblage fluctuations with major carbon-cycle perturbations through the early Eocene. Such correlation reveals that the remarkable planktic foraminiferal changes observed at Site 1263 are strongly related to the EECO and, at higher frequency, with the CIEs that preceded and continued to occur within the EECO (Fig. 5).

Comparisons to other locations where detailed foraminifera assemblage information and $\delta^{13}C$ records exist across the EECO (Frontalini et al., 2016; Luciani et al., 2016) shows some similarities and some differences. Specifically, we document a permanent drop in *Morozovella* abundance at Site 1263 (> 50%) slightly above the J event. We confirm, therefore, that the morozovellid decline recorded at low-latitude locations in the northern hemisphere (Frontalini et al., 2016; Luciani et al., 2016) can be found as well at a temperate latitude site in the southern hemisphere. However, the switch between the two dominant surface-dwellers, *Acarinina* and *Morozovella*, appears more gradual at Site 1263 and slightly delayed with respect to several other locations, where it occurs precisely at the J event (Luciani et al., 2016, in press). On the basis of the age model provided by Lauretano et al. (2016) for the Site 1263, we estimate the time of the decline began at ~53.05 Ma, or ~165 kyr after the J event (Fig. 6, Table 1). The pre-EECO mean relative abundance of the *Morozovella* at Site 1263 is lower (~23%, Fig. 5) than that recorded at the tropical Atlantic Site 1051 (~40%) and the tropical Pacific Site 577 (~30%) (Luciani et al., 2016). The lower morozovellid abundance at Site 1263 is probably related to

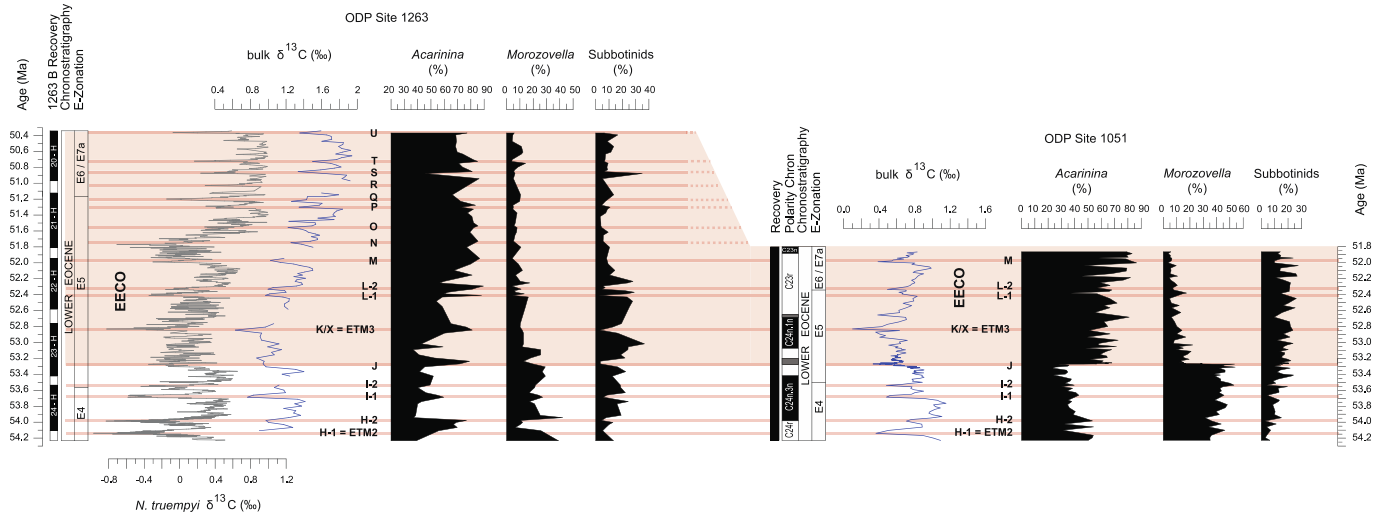

Fig. 6. Early Eocene $\delta^{13}C$ and primary planktic foraminiferal relative abundances from ODP sites 1263 and 1051 plotted versus Age (Ma). Age model is from option 2c of Lauretano et al. (2016) which is based on the tuning of two cycles of the long-eccentricity extracted from the orbital solution La2010d (Laskar et al. 2011). The $\delta^{13}C$ bulk sediment record at Site 1263 is from this study (blue) and benthic foraminiferal *N. truempyi* record comes from Lauretano et al. (2016) (grey). Bulk sediment $\delta^{13}C$ composition and planktic foraminiferal abundances from Site 1051 are from Luciani et al. (unpublished). Subbotinids include for both the sites the genera *Subbotina* (dominant) and *Parasubbotina* (very rare) that are known as having similar depth habitat (e.g., Pearson et al., 2006 and references therein). Other information is consistent with Fig. 2. Note the good correspondence between the two sites of the E4/E5 boundary, that is the B of *Morozovella aragonensis* and the marked diachronous E6/E7a boundary, that is the T of *Morozovella subbotinae*. Note also the slightly delayed decline of *Morozovella* abundance at Site 1263. (For interpretation of the references to colour in this figure legend, the reader is referred to the web version of this article.)

Table 1
Depth tie points between ODP Sites 1263B to 1051A and their relative ages according to the age model option 2c of Lauretano et al. (2016) which is based on the tuning of two long-eccentricity cycles extracted from the orbital solution La2010d (Laskar et al., 2011). Tie points coincide with the main negative carbon isotope excursions except for the basal and top points that correspond to positive $\delta^{13}C$ shifts.

CIE	Site 1263 B (rmcd)	Site 1051 A (mbsf)	Age (Kyr)
Positive $\delta^{13}C$ shift	261.05	390.60	51,866
M	262.90	396.10	51,988
L-2	268.20	406.70	52,335
L-1	269.08	409.80	52,392
K/X	275.08	417.30	52,831
J	280.80	428.34	53,270
I-2	285.22	439.08	53,538
I-1	287.72	443.13	53,685
H-2	292.92	450.67	53,986
H-1/ETM2	294.82	452.73	54,139
Positive $\delta^{13}C$ shift	295.76	454.18	54,228

mid-paleolatitude and relatively lower surface water temperature, given the surmised affinity for warm water of this genus (Boersma et al., 1987; Pearson et al., 2006 and reference therein). The slightly delayed drop in morozovellid abundance at Site 1263 demonstrates that during the EECO, when global temperatures peaked and other features changed in surface waters, unfavourable environmental conditions for morozovellids occurred at lower latitudes first.

3.6.3. Decline in chiloguembelinids and subbotinids and ecological niche reduction

The diverse planktic foraminiferal assemblages at Site 1263 include also relatively common occurrences of chiloguembelinids in the lower portion of the interval investigated. This supports the existence of a stratified water column in the pre-EECO interval with diverse ecological niches occupied. (Figs. 5, 7A). Chiloguembelinids decreased from ~10% of total foraminifera assemblages to become virtually and permanently absent above the K/X event. Multiple possible explanations for the chiloguembelinid disappearance can be forwarded. A possible interpretation involves the ecological behaviour of this group. Many Cenozoic biserial planktic foraminifera record light $\delta^{13}C$ values in conjunction with heavy $\delta^{18}O$ values compared to non-biserial surface dwelling planktic foraminifera (e.g., Boersma and Premoli Silva, 1989). This has led to the hypothesis that biserial planktic foraminifera were low-oxygen tolerant, meso- to eutrophic thermocline dwellers thriving in upwelling areas or were revealing the presence of a well-developed oxygen minimum zone (OMZ; Boersma et al., 1987; Boersma and Premoli Silva, 1989). These views were commonly accepted and adopted in paleoceanographic interpretations (e.g., Hallock et al., 1991; Luciani et al. 2007, 2010). The virtual chiloguembelinid disappearance within the EECO could therefore suggest a weakening of the OMZ (Fig. 7B), even though recent stable isotope analyses across the PETM suggest a higher than OMZ habitat within the lower mixed layer habitat for *Chiloguembelina wilcoxensis* and *Zeauvigerina* (D'haenens et al., 2012). Other analyses on *Chiloguembelina cubensis* from upper Eocene and Oligocene also indicate a surface or lower mixed layer (Poore and Matthews, 1984; Barrera and Huber, 1991, 1993; Zachos et al., 1992). New stable isotope data on early Eocene chiloguembelinids, yet absent, will help to clarify the true habitat preference of this group during this time interval.

Another possible explanation is that intermediate water temperatures also rose significantly during the EECO and conditions may have become too warm for this genus. A reduction in the thermocline-dwelling cold-index subbotinids (e.g., Boersma et al., 1987; Pearson et al., 1993, 2006), occurring above the paired L events, appears in line with the notion of thermocline warming at the EECO. It is unlikely that an increase in the relative abundance of *Subbotina senni*, which first appeared at the K/X event, counter-balanced the decrease in subbotinids in terms of ecological replacement, because the former taxon occupied a different habitat (Pearson et al., 1993; Pearson et al., 2006 and references therein). It is instead possible that this species, considered as a mixed-layer form that sank to middle mixed-layer or deeper depths during gametogenesis (above references), might have partly occupied the ecological niches released by morozovellids and/or chiloguembelinids.

The chiloguembelinids and subbotinids decline may have been a consequence of destratification of the upper water-column, whereby intermediate waters warmed relatively more than the surface waters. Interestingly, John et al. (2013, 2014), analyzing stable isotopes of lower and middle Eocene planktic foraminifera from Tanzania and Gulf of Mexico, conclude that there was a much greater temperature at

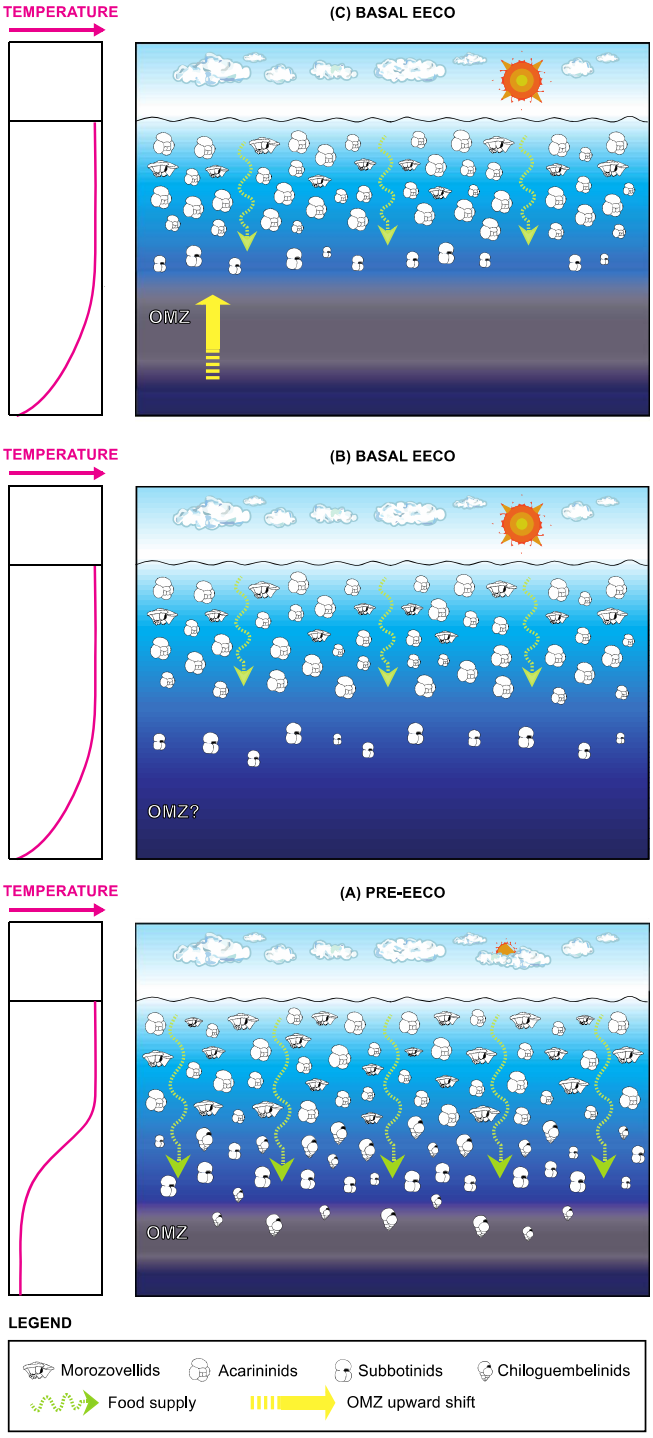

Fig. 7. Cartoons illustrating environmental changes across the EECO at Site 1263 in the upper water column as interpreted according to our record of changes in planktic foraminiferal assemblages. (A) Pre-EECO environment showing a well-stratified water column with morozovellids, chiloguembelinids and subbotinids still relatively abundant, stable food supply at depth and a relatively deep OMZ below the thermocline. (B) Basal EECO scenario showing increased acarininid and reduced subbotinid abundance. This may imply weakened water-column stratification related to enhanced warming in the thermocline. The virtual absence of chiloguembelinids could indicate weakening of the OMZ, according to the hypothesis that this group was low-oxygen tolerant (e.g., Boersma et al., 1987; Boersma and Premoli Silva, 1989). The possible causes for morozovellid decrease in abundance are discussed in the text. (C) Another option for the basal EECO scenario where contraction of the sub-surface and deeper dwelling niches of the eutrophic subbotinids and chiloguemeblinids was triggered by rapid and shallower bacterial remineralization due to intense warming causing an upward shift in the OMZ and reduced food supply at depth (John et al., 2013, 2014; Pearson and Coxall, 2014).

depths below the mixed layer. A further factor that may have inhibited the sub-surface taxa is related to the fact that elevated ocean temperatures enhanced the rate of bacterial respiration and remineralization significantly resulting in more efficient recycling of carbon and nutrients higher in the water column (John et al., 2013, 2014; Pearson and Coxall, 2014). This is consistent with the carbon isotope gradients that were steeper and larger through the upper thermocline during the early and middle Eocene than in the modern ocean (John et al., 2013, 2014). A more rapid and shallower bacterial remineralization would have contributed to an upward shift in the OMZ while food supply at depth was restricted which consequent cut out of the deeper dwelling niches in the lower thermocline (above references). Both subbotinids and chiloguembelinids, which are recognized as eutrophic taxa, thus may have suffered of reduced food supply besides the warmer temperatures (Fig. 7C). In this view, the new trophic and warmer state of the water column at the EECO damagingly prevailed on the presumed capacity to adapt to low-oxygen condition of chiloguembelinids and affected their abundance.

In conclusion, a contraction of the ecological niches may have occurred at Site 1263 in the sub-surface water and thermocline mainly driven by temperature increase.

3.6.4. High-frequency planktic foraminiferal variations during prominent CIEs

Short-term fluctuations in the relative abundances of the most common genera – *Acarinina*, *Morozovella* and *Subbotina* – coincide with the main CIEs (Fig. 5) and display anti-phase trends. Specifically, acarininids generally increase across the CIEs whereas morozovellids and subbotinids usually decrease and then suddenly recover above the events (Fig. 5). A different behaviour between the surface-dwelling acarininids and the thermocline-dwelling subbotinids might be expected. The opposing behaviour of *Morozovella* and *Acarinina*, which are known to share similar ecological affinities (e.g., Boersma et al., 1987; Pearson et al., 1993, 2006 and references therein), is intriguing. The striking dominance of *Acarinina* over *Morozovella* has been documented previously for the known early Eocene hyperthermals (PETM, ETM2/H-1 and K/X events) at several low-latitude successions from the Tethyan domain (Arenillas et al., 1999; Molina et al., 1999; Ernst et al., 2006; Guasti and Speijer, 2007; Luciani et al., 2007; Agnini et al., 2009; D'Onofrio et al., 2016; Luciani et al., 2016). This signal has been related to a transient rise in global temperature coupled with an increase in surface-water nutrient availability (above references). In turn, the latter has been attributed to an accelerated hydrological cycle and enhanced riverine discharge to continental margin settings during these events (e.g., Schmitz and Pujalte, 2007; Giusberti et al., 2007; Schulte et al., 2011; Slotnick et al., 2012, 2015; Pujalte et al., 2015). At Site 1263, well away from the continental margin, there is no evidence for greater terrigenous input or increased eutrophy. Our data highlight, therefore, that the anti-phase variation in *Acarinina* and *Morozovella* abundances is not restricted to the Tethyan domain or continental margin settings. Seemingly, it derives from a competition within the same mixed-layer, where acarininids tolerate the atypical conditions better (e.g., Luciani et al., 2007; Agnini et al., 2009; D'Onofrio et al., 2016; Luciani et al., 2016).

3.6.4.1. Causes of the permanent Morozovella decline. The triggering mechanism(s) of the permanent and widespread *Morozovella* decline at the EECO onset remain unknown. Increasingly, and as noted above, evidence suggests that competition between *Morozovella* and *Acarinina* played a significant role. We briefly summarize some hypotheses below.

The loss of algal photosymbionts has been thought to represent a potential mechanism to explain the rapid morozovellid decline at the start of the EECO (Luciani et al., 2016). This is because endosymbionts play an important role in certain planktic foraminifera, including calcification, longevity and growth, which allow the host to succeed in an oligotrophic environment (e.g., Bé, 1982; Bé et al., 1982; Hemleben

et al., 1989). Bleaching events have been suggested for large species of *Acarinina* and the genus *Morozovelloides*.

(morphologically and ecologically comparable with *Morozovella*) during the middle Eocene (Wade et al., 2008; Edgar et al., 2012).

A number of stressors that occurred during the long-lasting EECO may have caused the loss of endosymbionts (i.e., bleaching). These include prolonged and extreme warmth (Zachos et al., 2008; Bijl et al., 2009; Huber and Caballero, 2011; Hollis et al., 2012; Hönisch et al., 2012; Pross et al., 2012; Inglis et al., 2015) or possibly high pCO_2 and low surface-water pH (Pearson and Palmer, 2000; Fletcher et al., 2008; Lowenstein and Demicco, 2006; Zeebe et al., 2009; Smith et al., 2010; Hyland and Sheldon, 2013; Anagnostou et al., 2016). A bleaching hypothesis has been tested recently at the northwest Atlantic Site 1051 (Fig. 1) by measuring stable isotopes of different size fractions of multiple planktic foraminiferal genera and species (Luciani et al., unpublished). The results demonstrate that morozovellids indeed reduced their algal-symbiont relationships at the beginning of the EECO, but this was a transitory effect. Moreover, evidence for bleaching also occurred in the acarininids, but their relative abundance increased. Permanent loss of photosymbionts does not seem to be the main cause of the definitive morozovellid decline. Independent of bleaching, persistent changes in mixed-layer conditions, such as high temperature and different chemistry, may have contributed to an extended unfavourable habitat for morozovellid life and calcification. Interestingly, the decline in abundance is associated, for the morozovellids that mainly contributed to the decrease in abundance, with a test size reduction both at Site 1263 and Site 1051 (Luciani et al., unpublished). Several potential stressors may explain the reduced size and they may include, beside algal photosymbiont inhibition, changes in temperature, primary production, salinity and decrease in oxygen levels (e.g., Schmidt et al., 2004b, 2006). The concentrations of dissolved oxygen decreases in warm waters while protists require more life resources, such as oxygen and nutrients, because their metabolism accelerates when temperature increases (e.g., O'Connor et al., 2009). Thus, a strategy to optimize resource uptake is to enlarge surface area/volume ratio by reducing the cell mass and therefore the test-size (e.g., Atkinson et al., 2003). The species *M. lensiformis*, *M. aequa*, *M. subbotinae* and *M. marginodentata* may have reacted with morphological changes through their ecophenotypic plasticity to face the critical environmental imposed conditions, resulting in the observed test-size reduction.

An alternative explanation for the morozovellid decline includes competition with other microfossil groups (Luciani et al., 2016) or strengthened competition between *Morozovella* and *Acarinina*. As confirmed by the data at Site 1263, the anti-phase variations in *Acarinina* and *Morozovella* abundances are now recorded in different settings during the early Eocene hyperthermal events, as well as within and across the EECO. This strongly suggests competition between these two genera in the mixed-layer habitat during conditions of extreme warmth. Interestingly, most *Morozovella* species usually exhibit less extreme high $\delta^{13}C$ and low $\delta^{18}O$ values with respect to most acarininids. This feature has been found in examinations of Late Paleocene and Eocene foraminiferal assemblages (e.g., Shackleton et al., 1985; Boersma et al., 1987; Pearson et al., 2001; Quillévéré et al., 2001; John et al. 2013, 2014; Luciani et al., unpublished). Most morozovellids may have thus lived slightly deeper in the mixed-layer habitat or they may have sunk there at gametogenesis as suggests the occurrence of a late stage crust in the test and by the isotope values. These features are especially evident in *M. aragonensis*, *M. lensiformis* (John et al., 2013, 2014) and possibly in *M. aequa* and *M. subbotinae* (Luciani et al., unpublished). This is particular interesting because *M. aequa*, *M. subbotinae* and *M. lensiformis* appears to be as the species that largely contributed to the morozovellid decline at Site 1263. A more intense warming in the middle-lower mixed-layer with respect to the upper mixed-layer may have affected morozovellid reproduction at depth and reduced their abundance. This effect, transient during the relatively short-term hyperthermals, may have turned out to be detrimental during the prolonged extreme warming condition at the EECO. We can hypothesize therefore that the persisting EECO perturbation may have exceeded the optimal conditions over a sufficient duration of time to allow morozovellid proliferation and thus permitting acarininids to dominate the mixed-layer habitat.

4. Summary and conclusions

Our multiproxy records at Site 1263 provide new insights on planktic foraminiferal changes at the basal EECO from a temperate southern hemisphere setting. Quantitative analyses of planktic foraminiferal assemblages, carbon isotope based stratigraphy and dissolution proxies allow us to present new views on both long-term and short-term planktic foraminiferal fluctuations during the early Eocene. The main results can be summarized as follows.

(1) A distinct decline in the abundance of *Morozovella* and rise in the abundance of *Acarinina* happens at the beginning of the EECO, similar to as recorded at locations across low-latitudes in the northern hemisphere (Luciani et al., 2016; unpublished). This fundamental turnover in the dominant planktic foraminiferal genera was truly widely geographically widespread.

(2) The *Morozovella-Acarinina* switch is somewhat complicated in detail in terms of abundances and timing. Before the start of the EECO, mean abundances of *Morozovella* at Site 1263 are lower than those recorded at the tropical northern hemisphere sites (Luciani et al., 2016). Given the affinity of morozovellids to warm surface waters, this probably reflects paleo-latitude. The morozovellid decline at Site 1263 is also more gradual and delayed by ~165 kyr suggesting that unfavourable environmental conditions for morozovellids at the start of the EECO, such as sustained passage of a temperature threshold or other changes in surface waters, occurred at lower latitudes first.

(3) Three proxies for carbonate dissolution indicate that early Eocene planktic foraminiferal assemblages at Site 1263 are marginally affected by selective dissolution. Rather, the assemblage changes should mostly be interpreted in terms of changes in the mixed-layer. On this basis, we interpret the long-term decrease in WPCF values as relating to a reduction of planktic foraminiferal productivity across the EECO, which likely was associated with the decline in morozovellid abundance. Notably, the significant and permanent modifications to foraminiferal assemblages across the long-lasting EECO contrast to ephemeral changes during the hyperthermals earlier in the Eocene.

(4) The triggering mechanism for the striking planktic foraminiferal turnover remains elusive, because both *Morozovella* and *Acarinina* existed in the mixed-layer. The two genera may have had biological differences in their tolerance to temperature and ocean chemistry, such as pH. Reproduction of most morozovellids, that sank slightly deeper in the mixed-layer differently from most acarininids, may have hindered by warmer temperatures. Our data showing anti-phase variations in abundances during early Paleogene hyperthermals before the EECO strongly suggest that there was competition between *Morozovella* and *Acarinina*. In any case, and unlike the early Eocene hyperthermal events, the prolonged EECO perturbation may have exceeded optimal conditions for morozovellids, such that acarininids dominated surface-water habitats afterward.

(5) Along with the changes in the dominant planktic foraminiferal genera, changes occur in other, minor genera. There is a virtual disappearance of the biserial chiloguembelinids across the EECO, and a reduction in the abundance of the subbotinids. As these genera are linked to the sub-surface waters and thermocline, we interpret the environmental changes across the EECO as impacting the entire upper water-column, and producing contraction of ecological niches.

Acknowledgments

Data supporting this paper are available as in Tables S1–S3 in the supplementary information. Funding for this research was provided for

V.L. and R.D'O. by the Ferrara University (FAR Luciani 2016). G.D. was financially supported by the U.S. National Science Foundation (grant NSF-FESD-OCE-1338842), and B.W. was supported by UK Natural Environment Research Council (NERC) reference number NE/G014817, and Marie Curie Career Integration Grant "ERAS". Emily Walsh assisted with sample preparation at UCL. Samples were provided by the International Ocean Discovery Program (IODP). IODP is sponsored by the U.S. National Science Foundation and participating countries. We thank the Bremen Core Repository for handling our sample request. SEM images were acquired at the Centro di Microscopia Elettronica of the Ferrara University. We are grateful to the editor F. Marret-Davies, to P. Pearson and an anonymous reviewer who gave detailed and constructive reviews that improved the paper significantly.

Appendix A. Supplementary data

Supplementary data to this article can be found online at http://dx.doi.org/10.1016/j.gloplacha.2017.09.007.

References

Agnini, C., Muttoni, G., Kent, D.V., Rio, D., 2006. Eocene biostratigraphy and magnetic stratigraphy from Possagno, Italy: the calcareous nannofossil response to climate variability. Earth Planet. Sci. Lett. 241, 815–830. http://dx.doi.org/10.1016/j.epsl.2005.11.005.

Agnini, C., Backman, J., Brinkhuis, H., Fornaciari, E., Giusberti, L., Luciani, V., Rio, D., Sluijs, A., 2009. An early Eocene carbon cycle perturbation at similar to 52.5 Ma in the Southern Alps: chronology and biotic response. Paleoceanography 24, PA2209. http://dx.doi.org/10.1029/2008PA001649.

Agnini, C., Fornaciari, E., Raffi, I., Catanzariti, R., Pälike, H., Backman, J., Rio, D., 2014. Biozonation and biochronology of Paleogene calcareous nannofossils from low and middle latitudes. Newsl. Stratigr. 47 (2), 131–181. http://dx.doi.org/10.1127/0078-0421/2014/0042.

Anagnostou, E.H.J., Edgar, K.M., Foster, G.L., Ridgwell, A., Inglis, G.N., Pancost, R.D., Lunt, D.J., Pearson, P.N., 2016. Changing atmospheric CO_2 concentration was the primary driver of early Cenozoic climate. Nature 533, 380–384. http://dx.doi.org/10.1038/nature17423.

Arenillas, I., Molina, E., Schmitz, B., 1999. Planktic foraminiferal and $\delta^{13}C$ isotopic changes across the Paleocene/Eocene boundary at Possagno (Italy). Int. J. Earth Sci. 88, 352–364.

Arthur, M.A., Dean, W.E., Bottjer, D., Schole, P.A., 1984. Rhythmic bedding in Mesozoic-Cenozoic pelagic carbonate sequences: the primary and diagenetic origin of Milankovitch like cycles. In: Berger, A., Imbrie, J., Hays, J., Kucla, G., Satzman, B. (Eds.), Milankovitch and Climate. D. Reidel Publ. Company, Dordrecht, Holland, pp. 191–222.

Atkinson, D., Ciotti, B.J., Montagnes, D.J.S., 2003. Protists decrease in size linearly with temperature ca. 2.5% $^{\circ}C^{-1}$. Proc. R. Soc. Lond. B 270, 2605–2611. http://dx.doi.org/10.1098/rspb.2003.2538.

Aze, T., Ezard, T.H.G., Purvis, A., Coxall, H.K., Stewart, D.R.M., Wade, B.S., Pearson, P.N., 2011. A phylogeny of Cenozoic macroperforate planktonic foraminifera from fossil data. Biol. Rev. 86, 900–927. http://dx.doi.org/10.1111/j.1469-185X.2011.00178.x.

Barrera, E., Huber, B.T., 1991. Paleogene and early Neogene oceanography of the southern Indian Ocean: Leg 119 foraminifer stable isotope results. In: Barron, J.A., Larsen, B.L. (Eds.), Proceedings of the Ocean Drilling Program, Scientific Results: Ocean Drilling Program, College Station, TX 119. pp. 693–717.

Barrera, E., Huber, B.T., 1993. Eocene to Oligocene oceanography and temperatures in the Antarctic Indian Ocean. In: American Geophysical Union, Washington, D.C. 60. pp. 49–65.

Bé, A.W.H., 1982. Biology of planktonic foraminifera. In: Broadhead, T.W. (Ed.), Foraminifera: Notes for a Short Course (Stud. Geol., 6). Univ. Knoxville, Tenn, USA, pp. 51–92.

Bé, A.W.H., John, W.M., Stanley, M.H., 1975. Progressive dissolution and ultrastructural breakdown of planktic foraminifera. In: Cushman Foundation for Foraminiferal Research Special Publication 13. pp. 27–55.

Bé, A.W.H., Spero, H.J., Anderson, O.R., 1982. Effect of symbiont elimination and re-infection on the life processes of the planktonic foraminifera *Globigerinoides sacculifer*. Mar. Biol. 70, 73–86. http://dx.doi.org/10.1007/BF00397298.

Berger, W.H., 1970. Planktonic foraminifera — selective solution and lysocline. Mar. Geol. 8, 111–138.

Berger, W.H., 1973. Deep-sea carbonates: Pleistocene dissolution cycles. J. Foraminifer. Res. 3 (4), 187–195.

Berger, W.H., Bonneau, M.-C., Parker, F.L., 1982. Foraminifera on the deep-sea floor: lysocline and dissolution rate. Oceanol. Acta 5 (2), 249–258.

Berggren, W.A., Pearson, P.N., 2005. A revised tropical to subtropical Paleogene planktic foraminiferal zonation. J. Foraminifer. Res. 35, 279–298.

Berggren, W.A., Pearson, P.N., Huber, B.T., Wade, B.S., 2006. Taxonomy, biostratigraphy and phylogeny of Eocene Acarinina. In: Pearson, P.N., Olsson, R.K., Huber, B.T., Hemleben, C., Berggren, W.A. (Eds.), Atlas of Eocene Planktonic Foraminifera, Cushman Foundation Special Publication 41. pp. 257–326.

Bijl, P.K., Schouten, S., Sluijs, A., Reichart, G.-J., Zachos, J.C., Brinkhuis, H., 2009. Early Paleogene temperature evolution of the southwest Pacific Ocean. Nature 461, 776–779. http://dx.doi.org/10.1038/nature08399.

Boersma, A., Premoli Silva, I., 1989. Atlantic paleogene biserial heterohelicid foraminifera and oxygen minima. Paleoceanography 4 (3), 271–286. http://dx.doi.org/10.1029/PA004i003p00271.

Boersma, A., Premoli Silva, I., Shackleton, N., 1987. Atlantic Eocene planktonic foraminiferal biogeography and stable isotopic paleoceanography. Paleoceanography 2, 287–331.

Borre, M., Fabricus, I.L., 1998. Chemical and mechanical processes during burial diagenesis of chalk: an interpretation based on specific surface data of deep-sea sediments. Sedimentology 45, 755–769.

Coccioni, R., Bancalà, G., Catanzariti, R., Fornaciari, E., Frontalini, F., Giusberti, L., Jovane, L., Luciani, V., Savian, J., Sprovieri, M., 2012. An integrated stratigraphic record of the Palaeocene-lower Eocene at Gubbio (Italy), new insights into the early Palaeogene hyperthermals and carbon isotope excursions, Terra Nova, 24, 380–386. http://dx.doi.org/10.1111/j.1365-3121.2012.01076.x.

Corfield, R.M., 1987. Patterns of evolution in Palaeocene and Eocene planktonic foraminifera. In: Micropalaeontology of Carbonate Environments. Ellis Horwood, Chichester, England, pp. 93–110.

Cramer, B.S., Kent, D.V., Aubry, M.-P., 2003. Orbital climate forcing of excursions in the late Paleocene–early Eocene (chrons C24n–C25n). Paleoceanography 18 (4), 1097. http://dx.doi.org/10.1029/2003PA000909.

Dedert, M., Stoll, H., Kroon, D., Shimizu, N., Kanamaru, K., Ziveri, P., 2012. Productivity response of calcareous nannoplankton to Eocene Thermal Maximum 2 (ETM2). Clim. Pastoralism 8 (3), 977–993. http://dx.doi.org/10.5194/cp-8-977-2012.

Dedert, M., Stoll, H., Kars, S., Young, J.R., Shimizu, N., Kroon, D., Lourens, L., Ziveri, P., 2014. Temporally variable diagenetic overgrowth on deep-sea nannofossil carbonates across Palaeogene hyperthermals and implications for isotopic analyses. Mar. Micropaleontol. 107, 18–31. http://dx.doi.org/10.1016/j.marmicro.2012.02.006.

D'haenens, S., Bornemann, A., Roose, K., Claeys, P., Speijer, R., 2012. Stable isotope paleoecology ($\delta^{13}C$ and $\delta^{18}O$) of early Eocene *Zeauvigerina aegyptiaca* from the North Atlantic (DSDP Site 401). Aust. J. Earth Sci. 105 (1), 179–188.

D'haenens, S., Bornemann, A., Claeys, P., Röhl, U., Steurbaut, E., Speijer, R.P., 2014. A transient deep-sea circulation switch during Eocene Thermal Maximum 2. Paleoceanography 29, 370–388. http://dx.doi.org/10.1002/2013PA002567.

Dickens, G.R., Castillo, M., Walker, J.C.G., 1997. A blast of gas in the latest Paleocene: simulating first-order effects of massive dissociation of oceanic methane hydrate. Geology 25, 259–262.

D'Onofrio, R., Luciani, V., Giusberti, L., Fornaciari, E., Sprovieri, M., 2014. Tethyan planktic foraminiferal record of the early Eocene hyperthermal events ETM2, H2 and I1 (Terche section, northeastern Italy). Rend. Online Soc. Geol. Ital. 31, 66–67. http://dx.doi.org/10.3301/ROL.2014.48.

D'Onofrio, R., Luciani, V., Fornaciari, E., Giusberti, L., Boscolo Galazzo, F., Dallanave, E., Westerhold, T., Sprovieri, M., Telch, S., 2016. Environmental perturbations at the early Eocene ETM2, H2, and I1 events as inferred by Tethyan calcareous plankton (Terche section, northeastern Italy). Paleoceanography 31 (9), 1225–1247. http://dx.doi.org/10.1002/2016PA002940.

Edgar, K.M., Bohaty, S.M., Gibbs, S.J., Sexton, P.F., Norris, R.D., Wilson, P.A., 2012. Symbiont 'bleaching' in planktic foraminifera during the Middle Eocene Climatic Optimum. Geology 41, 15–18.

Ernst, S.R., Guasti, E., Dupuis, C., Speijer, R.P., 2006. Environmental perturbation in the southern Tethys across the Paleocene/Eocene boundary (Dababiya, Egypt): foraminiferal and clay mineral records. Mar. Micropaleontol. 60, 89–111. http://dx.doi.org/10.1016/j.marmicro.2006.03.002.

Ezard, T.H.G., Aze, T., Pearson, P.N., Purvis, A., 2011. Interplay between changing climate and species ecology drives macroevolutionary dynamics. Science 332, 349–351. http://dx.doi.org/10.1126/science.1203060.

Falkowski, P.G., Katz, M.E., Milligan, A.J., Fennel, K., Cramer, B.S., Aubry, M.P., Berner, R.A., Novacek, M.J., Zapol, W.M., 2005. The rise of oxygen over the past 205 million years and the evolution of large placental mammals. Science 309, 2202–2204. http://dx.doi.org/10.1126/science.1116047.

Figueirido, B., Janis, C., Pérez-Claros, M.J.A., De Renzi, M., Palmqvist, P., 2012. Cenozoic climate change influences mammalian evolutionary dynamics. Proc. Natl. Acad. Sci. U. S. A. 109, 722–727.

Fletcher, B.J., Brentnall, S.J., Anderson, C.W., Berner, R.A., Beerling, D.J., 2008. Atmospheric carbon dioxide linked with Mesozoic and early Cenozoic climate change. Nat. Geosci. 1, 43–48. http://dx.doi.org/10.1038/ngeo.2007.67.

Fraass, A.J., Kelly, D.K., Peters, S.E., 2015. Macroevolutionary history of the planktic foraminifera. Annu. Rev. Earth Planet. Sci. 43, 139–166. http://dx.doi.org/10.1146/annurev-earth-060614-105059.

Frank, T.D., Arthur, M.A., Dean, W.E., 1999. Diagenesis of Lower Cretaceous pelagic carbonates, North Atlantic: paleoceanographic signals obscured. J. Foraminifer. Res. 29, 340–351.

Frontalini, F., Coccioni, R., Catanzariti, R., Jovane, L., Savian, J.F., Sprovieri, M., 2016. The Eocene Thermal Maximum 3: reading the environmental perturbations at Gubbio (Italy). In: Geological Society of America Special Papers 524.

Gibbs, S.J., Bown, P.R., Murphy, B.H., Sluijs, A., Edgar, K.M., Pälike, H., Bolton, C.T., Zachos, J.C., 2012. Scaled biotic disruption during early Eocene global warming events. Biogeosciences 9 (11), 4679–4688. http://dx.doi.org/10.5194/bg-9-4679-2012.

Giusberti, L., Rio, D., Agnini, C., Backman, J., Fornaciari, E., Tateo, F., Oddone, M., 2007. Mode and tempo of the Paleocene–Eocene thermal maximum in an expanded section from the Venetian pre-Alps. Geol. Soc. Am. Bull. 119, 391–412. http://dx.doi.org/10.1130/B25994.1.

Green, O.R., 2001. A Manual of Practical Laboratory and Field Techniques in

Palaeobiology. Kluwer Academic, London 538 pp.
Guasti, E., Speijer, R.P., 2007. The Paleocene–Eocene thermal maximum in Egypt and Jordan: an overview of the planktic foraminiferal record. Geol. Soc. Spec. Pap. 424, 53–67.
Hallock, P., Premoli Silva, I., Boersma, A., 1991. Similarities between planktonic and larger foraminiferal evolutionary trends through Paleogene paleoceanographic changes. Palaeogeogr. Palaeoclimatol. Palaeoecol. 83, 43–64.
Hancock, H.J.L., Dickens, G.R., 2005. Carbonate dissolution episodes in Paleocene and Eocene sediment, Shatsky Rise, west-central Pacific. In: Bralower, T.J., Premoli Silva, I., Malone, M.J. (Eds.), Proceedings of the Ocean Drilling Program, Scientific Results 198. Texas A & M Univ., College Station, pp. 1–24. Available at World Wide Web. http://www-odp.tamu.edu/publications/198_SR/116/116.htm.
Hemleben, C., Spindler, M., Anderson, O.R. (Eds.), 1989. Modern Planktonic Foraminifera. Springer-Verlag, New York, pp. 1–363 ISBN-13: 9780387968155.
Hollis, C.J., Taylor, K.W.R., Handley, L., Pancost, R.D., Huber, M., Creech, J.B., Hines, B.R., Crouch, E.M., Morgans, H.E.G., Crampton, J.S., Gibbs, S., Pearson, P.N., Zachos, J.C., 2012. Early Paleogene temperature history of the Southwest Pacific Ocean: reconciling proxies and models. Earth Planet. Sci. Lett. 349–350, 53–66. http://dx.doi.org/10.1016/j.epsl.2012.06.024.
Hönisch, B., Ridgwell, A., Schmidt, D.N., Thomas, E., Gibbs, S.J., Sluijs, A., Zeebe, R., Kump, L., Martindale, R.C., Greene, S.E., Kiessling, W., Ries, J., Zachos, J.C., Royer, D.L., Barker, S., Marchitto Jr., T.M., Moyer, R., Pelejero, C., Ziveri, P., Foster, G.L., Williams, B., 2012. The geological record of ocean acidification. Science 335, 1058–1063. http://dx.doi.org/10.1126/science.1208277.
Huber, M., Caballero, R., 2011. The early Eocene equable climate problem revisited. Clim. Past 7, 603–633. http://dx.doi.org/10.5194/cp-7-603-2011.
Hyland, E.G., Sheldon, N.D., 2013. Coupled CO_2-climate response during the Early Eocene Climatic Optimum. Palaeogeogr. Palaeoclimatol. Palaeoecol. 369, 125–135. http://dx.doi.org/10.1016/j.palaeo.2012.10.011.
Inglis, G.N., Farnsworth, A., Lunt, D., Foster, G.L., Hollis, C.J., Pagani, M., Jardine, P.E., Pearson, P.N., Markwick, P., Galsworthy, A.M.J., Raynham, L., Taylor, K.W.R., Pancost, R.D., 2015. Descent toward the icehouse: Eocene sea surface cooling inferred from GDGT distributions. Paleoceanography 30, 100–1020. http://dx.doi.org/10.1002/2014PA002723.
John, E.H., Wilson, J.D., Pearson, P.N., Ridwell, A., 2013. Warm processes and carbon cycling in the Eocene. Philos. Trans. R. Soc. A Math. Phys. Eng. Sci. 371 (2001), 20130099. http://dx.doi.org/10.1098/rsta.2013.0099.
John, E.H., Pearson, P.N., Coxall, H.K., Birch, H., Wade, B.S., Foster, G.L., 2014. Temperature-dependent remineralization and carbon cycling in the warm Eocene oceans. Palaeogeogr. Palaeoclimatol. Palaeoecol. 413, 158–166. http://dx.doi.org/10.1016/j.palaeo.2014.05.019.
Kelly, D.C., Bralower, T.J., Zachos, J.C., Premoli Silva, I., Thomas, E., 1996. Rapid diversification of planktonic foraminifera in the tropical Pacific (ODP Site 865) during the late Paleocene thermal maximum. Geology 24, 423–426. http://dx.doi.org/10.1130/0091-7613(1996)024<0423:RDOPFI>2.3.CO;2.
Kelly, D.C., Bralower, T.J., Zachos, J.C., 1998. Evolutionary consequences of the latest Paleocene thermal maximum for tropical planktonic foraminifera. Palaeogeogr. Palaeoclimatol. Palaeoecol. 141, 139–161. http://dx.doi.org/10.1016/S0031-0182(98)00017-0.
Kennett, J.P., Stott, L.D., 1991. Abrupt deep-sea warming, palaeoceanographic changes and benthic extinctions at the end of the Palaeocene. Nature 353, 225–229. http://dx.doi.org/10.1038/353225a0.
Kirtland-Turner, S., Sexton, P.F., Charled, C.D., Norris, R.D., 2014. Persistence of carbon release events through the peak of early Eocene global warmth. Nat. Geosci. 7, 748–751. http://dx.doi.org/10.1038/NGEO2240.
Kozdon, R., Kelly, D.C., Kita, N.T., Fournelle, J.H., Valley, J.W., 2011. Planktonic foraminiferal oxygen isotope analysis by ion microprobe technique suggests warm tropical sea surface temperatures during the Early Paleogene. Paleoceanography 26, PA3206. http://dx.doi.org/10.1029/2010PA002056.
Kroenke, L.W., Berger, W.H., Janecek, T.R., Backman, J., Bassinot, F., Corfield, R.M., Delaney, M.L., Hagen, R., Jansen, E., Krissek, L.A., Lange, C., Leckie, R.M., Lykke Lind, I., Lyle, M.W., Mahoney, J.J., Marsters, J.C., Mayer, L., Mosher, D.C., Musgrave, R., Prentice, M.L., Resig, J.M., Schmidt, H., Stax, R., Storey, M., Takahashi, K., Takayama, T., Tarduno, J.A., Wilkens, R.H., Wu, G., Barbu, E.M., 1991. Ontong Java Plateau, Leg 130: synopsis of major drilling results. Proc. Ocean Drill. Program Init. Rep. 130, 497–537.
Kump, L., Bralower, T., Ridgwell, A., 2009. Ocean acidification in deep time. Oceanography 22, 94–107.
Laskar, J., Fienga, A., Gastineau, M., Manche, H., 2011. La2010: a new orbital solution for the long term motion of the Earth. Astron. Astrophys. 532, A89. http://dx.doi.org/10.1051/0004-6361/201116836.
Lauretano, V., Littler, K., Polling, M., Zachos, J.C., Lourens, L.J., 2015. Frequency, magnitude and character of hyperthermal events at the onset of the Early Eocene Climatic Optimum. Clim. Past 11, 1313–1324. http://dx.doi.org/10.5194/cp-11-1313-2015.
Lauretano, V., Hilgen, F.J., Zachos, J.C., Lourens, L.J., 2016. Astronomically tuned age model for the early Eocene carbon isotope events: a new high-resolution $\delta^{13}C$ benthic record of ODP Site 1263 between ~ 49 and ~ 54 Ma. Newsl. Stratigr. 49 (2), 383–400. http://dx.doi.org/10.1127/nos/2016/0077.
Leon-Rodriguez, L., Dickens, G.R., 2010. Constraints on ocean acidification associated with rapid and massive carbon injections: the early Paleogene record at ocean drilling program site 1215, equatorial Pacific Ocean. Palaeogeogr. Palaeoclimatol. Palaeoecol. 298 (3–4), 409–420. http://dx.doi.org/10.1016/j.palaeo.2010.10.029.
Littler, K., Röhl, U., Westerhold, T., Zachos, J.C., 2014. A high-resolution benthic stable isotope record for the South Atlantic: implications for orbital-scale changes in late Paleocene–early Eocene climate and carbon cycling. Earth Planet. Sci. Lett. 401, 18–30. http://dx.doi.org/10.1016/j.epsl.2014.05.054.
Lourens, L.J., Sluijs, A., Kroon, D., Zachos, J.C., Thomas, E., Röhl, U., Bowles, J., Raffi, I., 2005. Astronomical pacing of late Palaeocene to early Eocene global warming events. Nature 435, 1083–1087. http://dx.doi.org/10.1038/nature03814.
Lowenstein, T.K., Demicco, R.V., 2006. Elevated Eocene atmospheric CO_2 and its subsequent decline. Science 313, 1928. http://dx.doi.org/10.1126/science.1129555.
Lu, G., Keller, G., 1995. Planktic foraminiferal faunal turnovers in the subtropical Pacific during the late Paleocene to early Eocene. J. Foraminifer. Res. 25, 97–116.
Luciani, V., Giusberti, L., 2014. Reassessment of the early–middle Eocene planktic foraminiferal biomagnetochronology: new evidence from the Tethyan Possagno section (NE Italy) and Western North Atlantic Ocean ODP Site 1051. J. Foraminifer. Res. 44, 187–201.
Luciani, V., Giusberti, L., Agnini, C., Backman, J., Fornaciari, E., Rio, D., 2007. The Paleocene–Eocene Thermal Maximum as recorded by Tethyan planktonic foraminifera in the Forada section (northern Italy). Mar. Micropaleontol. 64 (3), 189–214. http://dx.doi.org/10.1016/j.marmicro.2007.05.001.
Luciani, V., Giusberti, L., Agnini, C., Fornaciari, E., Rio, D., Spofforth, D.J.A., Pälike, H., 2010. Ecological and evolutionary response of Tethyan planktonic foraminifera to the middle Eocene climatic optimum (MECO) from the Alano section (NE Italy). Palaeogeogr. Palaeoclimatol. Palaeoecol. 292, 82–95. http://dx.doi.org/10.1016/j.palaeo.2010.03.029.
Luciani, V., Dickens, G.R., Backman, J., Fornaciari, E., Giusberti, L., Agnini, C., D'Onofrio, R., 2016. Major perturbations in the global carbon cycle and photosymbiont-bearing planktic foraminifera during the early Eocene. Clim. Past 12, 981–1007. http://dx.doi.org/10.5194/cp-12-981-2016.
Luciani, V., D'Onofrio, R., Dickens, J.R., Wade, B.S., 2017. Did photosymbiont bleaching lead to the demise of planktic foraminifer *Morozovella* at the Early Eocene Climatic Optimum? Paleoceanogra. Paleoclimatol in press.
Luo, Y., Boudreau, B.P., Dickens, G.R., Sluijs, A., Middelburg, J.J., 2016. An alternative model for $CaCO_3$ over-shooting during the PETM: biological carbonate compensation. Earth Planet. Res. Lett. 453, 223–233.
Matter, A., Douglas, R.G., Perch-Nielsen, K., 1975. Fossil preservation, geochemistry and diagenesis of pelagic carbonates from Shatsky Rise, northwest Pacific. Initial Rep. Deep Sea 32, 891–922. http://dx.doi.org/10.2973/dsdp.proc.32.137.1975.
McInerney, F.A., Wing, S.L., 2011. The Paleocene-Eocene Thermal Maximum: a perturbation of carbon cycle, climate, and biosphere with implications for the future. Annu. Rev. Earth Planet. Sci. 39 (1), 489–516. http://dx.doi.org/10.1146/annurev-earth-040610-133431.
Molina, E., Arenillas, I., Pardo, A., 1999. High resolution planktic foraminiferal biostratigraphy and correlation across the Palaeocene/Eocene boundary in the Tethys. B. Soc. Géol. Fr. 170, 521–530.
Molina, E., Alegret, L., Apellaniz, E., Bernaola, G., Caballero, F., Dinarès-Turell, J., Hardenbol, J., Heilmann-Clausen, C., Larrasoaña, J.C., Luterbacher, H., Monechi, S., Ortiz, S., Orue-Etxebarria, X., Payros, A., Pujalte, V., Rodríguez-Tovar, F.J., Tori, F., Tosquella, F., Uchman, A., 2011. The Global Stratotype Section and Point (GSSP) for the base of the Lutetian Stage at the Gorrondatxe section, Spain. Episodes 34, 86–108.
Murray, J.W., 1976. A method of determining proximity of marginal seas to an ocean. Mar. Geol. 22, 103–119.
Nguyen, T.M.P., Speijer, R.P., 2014. A new procedure to assess dissolution based on experiments on Pliocene–Quaternary foraminifera (ODP Leg 160, Eratosthenes Seamount, Eastern Mediterranean). Mar. Micropaleontol. 106, 22–39. http://dx.doi.org/10.1016/j.marmicro.2013.11.004.
Nguyen, T.M.P., Petrizzo, M.-R., Speijer, R.P., 2009. Experimental dissolution of a fossil foraminiferal assemblage (Paleocene–Eocene Thermal Maximum, Dababiya, Egypt): implications for paleoenvironmental reconstructions. Mar. Micropaleontol. 73 (3–4), 241–258. http://dx.doi.org/10.1016/j.marmicro.2009.10.005.
Nguyen, T.M.P., Petrizzo, M.-R., Stassen, P., Speijer, R.P., 2011. Dissolution susceptibility of Paleocene–Eocene planktic foraminifera: implications for palaeoceanographic reconstructions. Mar. Micropaleontol. 81 (1–2), 1–21. http://dx.doi.org/10.1016/j.marmicro.2011.07.001.
Nicolo, M.J., Dickens, G.R., Hollis, C.J., Zachos, J.C., 2007. Multiple early Eocene hyperthermals: their sedimentary expression on the New Zealand continental margin and in the deep sea. Geology 35 (8), 699–702. http://dx.doi.org/10.1130/G23648A.
Norris, R.D., 1991. Biased extinction and evolutionary trends. Paleobiology 17, 388–399.
O'Connor, M., Piehler, M.F., Leech, D.M., Anton, A., Bruno, J.F., 2009. Warming and resource availability shift food web structure and metabolism. PLoS Biol. 7 (8), 1–6. http://dx.doi.org/10.1371/journal.pbio.1000178.
Oreshkina, T.V., 2012. Evidence of late Paleocene–early Eocene hyperthermal events in biosiliceous sediments of Western Siberia and adjacent areas. Aust. J. Earth Sci. 105, 145–153.
Pagani, M., Caldeira, K., Archer, D., Zachos, J.C., 2006. An ancient carbon mystery. Science 314, 1556–1557. http://dx.doi.org/10.1126/science.1136110.
Pearson, P.N., 2012. Oxygen isotopes in foraminifera: overview and historical review, in reconstructing Earth's deep-time climate—the state of the art in 2012, paleontological society short course, November 3, 2012. In: Ivany, Linda C., Huber, Brian T. (Eds.), The Paleontological Society Papers 18. pp. 1–38.
Pearson, P.N., Coxall, H.K., 2014. Origin of the Eocene planktonic foraminifer Hantkenina by gradual evolution. Palaeontology 57 (2), 243–267. http://dx.doi.org/10.1111/pala.12064.
Pearson, P.N., Palmer, M.R., 2000. Atmospheric carbon dioxide concentrations over the past 60 million years. Nature 406 (6797), 695–699.
Pearson, P.N., Shackleton, N.J., Hall, M.A., 1993. Stable isotope paleoecology of middle Eocene planktonic foraminifera and multispecies isotope stratigraphy, DSDP Site 523, South Atlantic. J. Foraminifer. Res. 23, 123–140. http://dx.doi.org/10.2113/gsjfr.23.2.123.
Pearson, P.N., Ditchfield, P.W., Singano, J., Harcourt-Brown, K.G., Nicholas, C.J., Olsson,

R.K., Shackleton, N.J., Hall, M.A., 2001. Warm tropical sea surface temperatures in the Late Cretaceous and Eocene epochs. Nature 413, 481–487. http://dx.doi.org/10.1038/35097000.

Pearson, P.N., Olsson, R.K., Hemblen, C., Huber, B.T., Berggren, W.A. (Eds.), 2006. Atlas of Eocene planktonic foraminifera. Cushman Special Publication 41. Department of Geology East Carolina Univ., Greenville, pp. 513.

Petrizzo, M.-R., Leoni, G., Speijer, R.P., De Bernardi, B., Felletti, F., 2008. Dissolution susceptibility of some Paleogene planktonic foraminifera from ODP Site 1209 (Shatsky Rise, Pacific Ocean). J. Foraminifer. Res. 38 (4), 357–371. http://dx.doi.org/10.1016/j.marmicro.2011.07.001.

Poore, R.Z., Matthews, R.K., 1984. Oxygen isotope ranking of Late Eocene and Oligocene planktonic foraminifers: implications for Oligocene sea-surface temperature and global ice volume. Mar. Micropaleontol. 9, 111–134.

Pross, J., Contreras, L., Bijl, P.K., Greenwood, D.R., Bohaty, S.M., Schouten, S., Bendle, J.A., Röhl, U., Tauxe, L., Raine, J.I., Claire, E., Huck, C.E., van de Flierdt, T., Stewart, S.R., Jamieson, S.S.R., Stickley, C.E., van de Schootbrugge, B., Escutia, C., Brinkhuis, H., 2012. Persistent near-tropical warmth on the Antarctic continent during the early Eocene Epoch. Nature 488, 73–77. http://dx.doi.org/10.1038/nature11300.

Pujalte, V., Baceta, J.I., Schmitz, B., 2015. A massive input of coarse-grained siliciclastics in the Pyrenean Basin during the PETM: the missing ingredient in a coeval abrupt change in hydrological regime. Clim. Past 11 (12), 1653–1672. http://dx.doi.org/10.5194/cp-11-1653-2015.

Quillévéré, F., Norris, R.D., 2003. Ecological development of acarininids (planktonic foraminifera) and hydrographic evolution of Paleocene surface waters. In: Special Papers-Geological Society of America, pp. 223–238.

Quillévéré, F., Norris, R.D., Moussa, I., Berggren, W.A., 2001. Role of photosymbiosis and biogeography in the diversification of early Paleogene acarininids (planktonic foraminifera). Paleobiology 27 (2), 311–326. http://dx.doi.org/10.1666/0094-8373(2001)027<0311:ROPABI>2.0.CO;2.

Reghellin, D., Dickens, G.R., Backman, J., 2013. The relationship between wet bulk density and carbonate content in sediments from the Eastern Equatorial Pacific. Mar. Geol. 344, 41–52. http://dx.doi.org/10.1016/j.margeo.2013.07.007.

Schlanger, S.O., Douglas, R.G., 1974. The pelagic ooze-chalk limestone transition and its implications for marine stratigraphy, in pelagic sediments: on land and under the sea. In: Hsü, K.J., Jenkyns, H.C. (Eds.), Sp. Publ. Int. 1. pp. 117–148.

Schmidt, D.N., Renaud, S., Bollmann, J., Schiebel, R., Thierstein, H.R., 2004a. Size distribution of Holocene planktic foraminifer assemblages: biogeography, ecology and adaptation. Mar. Micropaleont. 50 (3–4), 319–338. http://dx.doi.org/10.1016/S0377-8398(03)00098-7.

Schmidt, D.N., Thierstein, H.R., Bollmann, J., 2004b. The evolutionary history of size variation of planktic foraminiferal assemblages in the Cenozoic. Palaeogeogr. Palaeoclimatol. Palaeoecol. 212, 159–180.

Schmidt, D.N., Lazarus, D., Young, J.R., Kucera, M., 2006. Biogeography and evolution of body size in marine plankton. Earth Sci. Rev. 78, 239–266. http://dx.doi.org/10.1016/j.earscirev.2006.05.004.

Schmitz, B., Pujalte, V., 2007. Abrupt increase in seasonal extreme precipitation at the Paleocene-Eocene boundary. Geology 35, 215–218. http://dx.doi.org/10.1130/G23261A.1.

Schneider, L.J., Bralower, T.J., Kump, L.J., 2011. Response of nannoplankton to early Eocene ocean destratification. Palaeogeogr. Palaeoclimatol. Palaeoecol 310, 152–162. http://dx.doi.org/10.1016/j.palaeo.2011.06.018.

Schrag, D.P., Depaolo, D.J., Richter, F.M., 1995. Reconstructing past sea surface temperatures: correcting for diagenesis of bulk marine carbonate. Geochim. Cosmochim. Acta 59, 2265–2278. http://dx.doi.org/10.1016/0016-7037(95)00105-9.

Schulte, P., Scheibner, C., Speijer, R.C., 2011. Fluvial discharge and sea-level changes controlling black shale deposition during the Paleocene–Eocene Thermal Maximum in the Dababiya Quarry section, Egypt. Chem. Geol. 285, 167–183. http://dx.doi.org/10.1016/j.chemgeo.2011.04.004.

Sexton, P.F., Wilson, P.A., Pearson, P.N., 2006. Microstructural and geochemical perspectives on planktic foraminiferal preservation: 'Glassy' versus 'Frosty'. Geochem. Geophys. Geosyst. 7, Q12P19. http://dx.doi.org/10.1029/2006GC001291.

Shackleton, N.J., Corfield, R.M., Hall, M.A., 1985. Stable isotope data and the ontogeny of Paleocene planktonic foraminifera. J. Foraminifer. Res. 15 (4), 321–336.

Shamrock, J.L., Watkins, D.K., Johnston, K.W., 2012. Eocene biogeochronology and magnetostratigraphic revision of ODP Hole 762C, Exmouth Plateau (northwest Australian Shelf). Stratigraphy 9 (1), 55.

Shipboard Scientific Party, 2004. Site 1263. In: Zachos, J.C., Kroon, D., Blum, P. (Eds.), Proc. ODP, Init. Repts., 208, College Station, TX (Ocean Drilling Program), pp. 1–87. http://dx.doi.org/10.2973/odp.proc.ir.208.104.2004.

Sims, P.A., Mann, D.G., Medlin, L.K., 2006. Evolution of the diatoms: insights from fossil, biological and molecular data. Phycologia 45 (4), 361–402.

Slotnick, B.S., Dickens, G.R., Nicolo, M.J., Hollis, C.J., Crampton, J.S., Zachos, J.C., 2012. Large-amplitude variations in carbon cycling and terrestrial weathering during the latest Paleocene and earliest Eocene: the record at Mead Stream, New Zealand. J. Geol. 120 (5), 487–505. http://dx.doi.org/10.1086/666743.

Slotnick, B.S., Dickens, G.R., Hollis, C.J., Crampton, J.S., Strong, P.S., Phillips, A., 2015. The onset of the Early Eocene climatic optimum at branch stream, Clarence Rivervalley, New Zealand. J. Geol. Geophys. 58, 1–19. http://dx.doi.org/10.1080/00288306.2015.1063514.

Smith, R.Y., Greenwood, D.R., Basinger, J.F., 2010. Estimating paleoatmospheric pCO_2 during the early Eocene climatic optimum from stomatal frequency of ginkgo, Okanagan highlands, British Columbia, Canada. Palaeogeogr. Palaeoclimatol. Palaeoecol. 293, 120–131. http://dx.doi.org/10.1016/j.palaeo.2010.05.006.

Stap, L., Sluijs, A., Thomas, E., Lourens, L.J., 2009. Patterns and magnitude of deep sea carbonate dissolution during Eocene Thermal Maximum 2 and H2, Walvis Ridge, Southeastern Atlantic Ocean. Paleoceanography 24, PA1211. http://dx.doi.org/10.1029/2008PA001655.

Stap, L., Lourens, L.J., Thomas, E., Sluijs, A., Bohaty, S., Zachos, J.C., 2010a. High-resolution deep-sea carbon and oxygen isotope records of Eocene Thermal Maximum 2 and H2. Geology 38, 607–610. http://dx.doi.org/10.1130/G30777.1.

Stap, L., Lourens, L.J., van Dijk, A., Schouten, S., Thomas, E., 2010b. Coherent pattern and timing of the carbon isotope excursion and warming during Eocene Thermal Maximum 2 as recorded in planktic and benthic foraminifera. Geochem. Geophys. Geosyst. 11, Q11011. http://dx.doi.org/10.1029/2010GC003097.

Thomas, E., Zachos, J.C., Bralower, T.J., 2000. Deep-sea environments on a warm Earth: latest Paleocene–early Eocene. In: Huber, B., MacLeod, K., Wing, S. (Eds.), Warm Climates in Earth History. Cambridge Univ. Press, Cambridge, U. K., pp. 132–160.

Thunell, R.C., Honjo, S., 1981. Calcite dissolution and the modification of planktonic foraminiferal assemblages. Mar. Micropaleontol. 6 (2), 169–182.

Van der Zwaan, G.J., Jorissen, F.J., De Stigter, H.C., 1990. The depth dependency of planktonic/benthic foraminiferal ratios: constraints and applications. Mar. Geol. 95 (1), 1–16.

Van Hinsbergen, D.J.J., de Groot, L.V., van Schaik, S.J., Spakman, W., Bijl, P.K., Sluijs, A., Langereis, C.G., Brinkhuis, H., 2015. A paleolatitude calculator for paleoclimate studies. PLoS One 10, e0126946. http://dx.doi.org/10.1371/journal.pone.0126946.

Wade, B.S., Al-Sabouni, N., Hemleben, C., Kroon, D., 2008. Symbiont bleaching in fossil planktonic foraminifera. Evol. Ecol. 22, 253–265. http://dx.doi.org/10.1007/s10682-007-9176-6.

Wade, B.S., Pearson, P.N., Berggren, W.A., Pälike, H., 2011. Review and revision of Cenozoic tropical planktonic foraminiferal biostratigraphy and calibration to the geomagnetic polarity and astronomical time scale. Earth Sci. Rev. 104 (1–3), 111–142. http://dx.doi.org/10.1016/j.earscirev.2010.09.003.

Westerhold, T., Röhl, U., Laskar, J., Raffi, I., Bowles, J., Lourens, L.J., Zachos, J.C., 2007. On the duration of magnetochrons C24r and C25n and the timing of early Eocene global warming events: implications from the Ocean Drilling Program Leg 208 Walvis Ridge depth transect. Paleoceanography 22, PA2201. http://dx.doi.org/10.1029/2006PA001322.

Westerhold, T., Röhl, U., Frederichs, T., Bohaty, S.M., Zachos, J.C., 2015. Astronomical calibration of the geological timescale: closing the middle Eocene gap. Clim. Past 11 (9), 1181–1195. http://dx.doi.org/10.5194/cp-11-1181-2015.

Wilf, P., Cúneo, R.N., Johnson, K.R., Hicks, J.F., Wing, S.L., Obradovich, J.D., 2003. High plant diversity in Eocene South America: evidence from Patagonia. Science 300, 122–125. http://dx.doi.org/10.1126/science.1080475.

Wing, S.L., Bown, T.M., Obradovich, J.D., 1991. Early Eocene biotic and climatic change in interior western North America. Geology 19, 1189–1192.

Woodburne, M.O., Gunnell, G.F., Stucky, R.K., 2009. Climate directly influences Eocene mammal faunal dynamics in North America. Proc. Natl. Acad. Sci. U. S. A. 106, 13399–13403.

Zachos, J.C., Berggren, W.A., Aubry, M.P., Mackenses, A., 1992. Isotope and trace element geochemistry of Eocene and Oligocene foraminifers from Site 748, Kerguelen Plateau. Proc. Ocean Drill. Program Sci. Results 120, 839–854.

Zachos, J.C., Pagani, M., Sloan, L., Thomas, E., Billups, K., 2001. Trends, rhythms, and aberrations in global climate 65 Ma to present. Science 292, 686–693. http://dx.doi.org/10.1126/science.1059412.

Zachos, J.C., Kroon, D., Blum, P., et al., 2004. Proc. ODP, Init. Repts., 208: College Station, TX (Ocean Drilling Program). http://dx.doi.org/10.2973/odp.proc.ir.208.2004.

Zachos, J.C., Röhl, U., Schellenberg, S.A., Sluijs, A., Hodell, D.A., Kelly, D.C., Thomas, E., Nicolo, M., Raffi, I., Lourens, L.J., McCarren, H., Kroon, D., 2005. Rapid acidification of the ocean during the Paleocene–Eocene thermal maximum. Science 308, 1611–1615. http://dx.doi.org/10.1126/science.1109004.

Zachos, J.C., Dickens, G.R., Zeebe, R.E., 2008. An early Cenozoic perspective on greenhouse warming and carbon-cycle dynamics. Nature 451 (7176), 279–283. http://dx.doi.org/10.1038/nature06588.

Zachos, J.C., McCarren, H.K., Murphy, B., Röhl, U., Westerhold, T., 2010. Tempo and scale of late Paleocene and early Eocene carbon isotope cycles: implications for the origin of hyperthermals. Earth Planet. Sci. Lett. 299, 242–249. http://dx.doi.org/10.1016/j.epsl.2010.09.004.

Zeebe, R.E., Zachos, J.C., 2013. Long-term legacy of massive carbon input to the Earth system: Anthropocene versus Eocene. Philos. Trans. R. Soc. Lond. A Math. Phys. Eng. Sci. 371 (2001), 20120006.

Zeebe, R.E., Zachos, J.C., Dickens, G.R., 2009. Carbon dioxide forcing alone insufficient to explain Palaeocene–Eocene Thermal Maximum warming. Nat. Geosci. 2 (8), 576–580. http://dx.doi.org/10.1038/ngeo578.

Zonneveld, J.P., Gunnell, G.F., Bartels, W.S., 2000. Early Eocene fossil vertebrates from the southwestern Green River Basin, Lincoln and Uinta Counties, Wyoming. J. Vertebr. Paleontol. 20, 369–386.